JCI The Journal of Clinical Investigation

CD4$^+$CD25$^+$Foxp3$^+$ Tregs resolve experimental lung injury in mice and are present in humans with acute lung injury

Franco R. D'Alessio, Kenji Tsushima, Neil R. Aggarwal, Erin E. West, Matthew H. Willett, Martin F. Britos, Matthew R. Pipeling, Roy G. Brower, Rubin M. Tuder, John F. McDyer, Landon S. King

J Clin Invest. 2009;119(10):2898-2913. https://doi.org/10.1172/JCI36498.

Research Article

Acute lung injury (ALI) is characterized by rapid alveolar injury, inflammation, cytokine induction, and neutrophil accumulation. Although early events in the pathogenesis of ALI have been defined, the mechanisms underlying resolution are unknown. As a model of ALI, we administered intratracheal (i.t.) LPS to mice and observed peak lung injury 4 days after the challenge, with resolution by day 10. Numbers of alveolar lymphocytes increased as injury resolved. To examine the role of lymphocytes in this response, lymphocyte-deficient *Rag-1*$^{-/-}$ and C57BL/6 WT mice were exposed to i.t. LPS. The extent of injury was similar between the groups of mice through day 4, but recovery was markedly impaired in the *Rag-1*$^{-/-}$ mice. Adoptive transfer studies revealed that infusion of CD4$^+$CD25$^+$Foxp3$^+$ Tregs as late as 24 hours after i.t. LPS normalized resolution in *Rag-1*$^{-/-}$ mice. Similarly, Treg depletion in WT mice delayed recovery. Treg transfer into i.t. LPS–exposed *Rag-1*$^{-/-}$ mice also corrected the elevated levels of alveolar proinflammatory cytokines and increased the diminished levels of alveolar TGF-β and neutrophil apoptosis. Mechanistically, Treg-mediated resolution of lung injury was abrogated by TGF-β inhibition. Moreover, BAL of patients with ALI revealed dynamic changes in CD3$^+$CD4$^+$CD25^{hi}CD127^{lo}Foxp3$^+$ cells. These results indicate that Tregs modify innate immune responses during resolution of lung injury and suggest potential targets for treating ALI, for which there are no specific therapies currently […]

 Related Commentary, page 2891

CD4+CD25+Foxp3+ Tregs resolve experimental lung injury in mice and are present in humans with acute lung injury

Franco R. D'Alessio,[1] Kenji Tsushima,[1] Neil R. Aggarwal,[1] Erin E. West,[1] Matthew H. Willett,[1] Martin F. Britos,[1] Matthew R. Pipeling,[1] Roy G. Brower,[1] Rubin M. Tuder,[1,2] John F. McDyer,[1] and Landon S. King[1]

[1]Division of Pulmonary and Critical Care Medicine, Department of Medicine, and
[2]Department of Pathology, Johns Hopkins University School of Medicine, Baltimore, Maryland, USA.

Acute lung injury (ALI) is characterized by rapid alveolar injury, inflammation, cytokine induction, and neutrophil accumulation. Although early events in the pathogenesis of ALI have been defined, the mechanisms underlying resolution are unknown. As a model of ALI, we administered intratracheal (i.t.) LPS to mice and observed peak lung injury 4 days after the challenge, with resolution by day 10. Numbers of alveolar lymphocytes increased as injury resolved. To examine the role of lymphocytes in this response, lymphocyte-deficient *Rag-1*$^{-/-}$ and C57BL/6 WT mice were exposed to i.t. LPS. The extent of injury was similar between the groups of mice through day 4, but recovery was markedly impaired in the *Rag-1*$^{-/-}$ mice. Adoptive transfer studies revealed that infusion of CD4$^+$CD25$^+$Foxp3$^+$ Tregs as late as 24 hours after i.t. LPS normalized resolution in *Rag-1*$^{-/-}$ mice. Similarly, Treg depletion in WT mice delayed recovery. Treg transfer into i.t. LPS–exposed *Rag-1*$^{-/-}$ mice also corrected the elevated levels of alveolar proinflammatory cytokines and increased the diminished levels of alveolar TGF-β and neutrophil apoptosis. Mechanistically, Treg-mediated resolution of lung injury was abrogated by TGF-β inhibition. Moreover, BAL of patients with ALI revealed dynamic changes in CD3$^+$CD4$^+$CD25^{hi}CD127^{lo}Foxp3$^+$ cells. These results indicate that Tregs modify innate immune responses during resolution of lung injury and suggest potential targets for treating ALI, for which there are no specific therapies currently available.

Introduction

Acute lung injury (ALI), a syndrome of rapid-onset bilateral pulmonary infiltrates of noncardiac origin, is characterized by alveolar-capillary injury, inflammation with neutrophil accumulation, and release of proinflammatory cytokines (1). ALI can result in persistent respiratory failure and prolonged dependence on mechanical ventilation, increasing susceptibility to multiorgan dysfunction and mortality. ALI produces nearly 200,000 hospitalizations and 75,000 deaths in the United States each year (2). Despite extensive investigation aimed at early diagnostic and pathogenetic factors of ALI, current management is mainly supportive, as specific therapies have not been identified. Animal models focused on early events (24–48 hours) in ALI pathogenesis have yielded insights into mechanisms that initiate injury; however, little is known about potential determinants of resolution.

Injury resolution is an active process (3) that requires a series of integrated steps including transitions in the balance of pro- and antiinflammatory cytokines, as well as clearance of neutrophils from sites of inflammation (4–6). Similar events are likely required to achieve resolution of ALI. Lymphocytes have been implicated in regulation of numerous inflammatory, autoimmune, and allergic conditions (7–9), as well as in protection against experimental bacterial sepsis (10); however, potential roles for lymphocytes in the pathogenesis or resolution of ALI have not been described. A subset of CD4$^+$ lymphocytes described as Tregs, expressing the surface marker CD25 (IL-2 receptor α) as well as the transcription factor Forkhead box protein 3 (Foxp3), have been implicated in controlling autoreactive T cells in vivo (11). Recent reports indicate that Tregs exert suppressive effects in an increasing array of pathophysiologic events (12, 13), including regulation of immune responses after burn injury in mice (14) and in chronic infections such as pulmonary aspergillosis (15) and *Pneumocystis pneumonia* (16), and therefore might participate as mediators in ALI or its resolution.

Using a well-established model of lung injury, intratracheal (i.t.) LPS, we identified a critical role for Tregs in resolution of ALI. Lymphocyte-deficient recombinase activating gene–1–null (*Rag-1*$^{-/-}$) mice (17) exhibited a profound impairment in resolution of lung injury that was reversed by administration of isolated Tregs, and depletion of Tregs in WT mice delayed recovery. In the absence of Tregs, LPS-induced proinflammatory responses were sustained, and neutrophil apoptosis was reduced. TGF-β, but not IL-10, was required to achieve Treg-mediated resolution of ALI. In addition, we identified the presence of human Tregs (CD3$^+$CD4$^+$CD25$^+$CD127^{lo}Foxp3$^+$) in BAL in 2 patients who met clinical-radiological criteria (18, 19) for ALI. Our results provide evidence of an integral role for Tregs in resolution of ALI, which we believe to be novel, as well as evidence for cross-talk between innate and adaptive immune systems in the transition from injury to repair in the lung.

Results

Resolution of lung injury is impaired in lymphocyte-deficient mice. In preliminary studies, we investigated alveolar inflammatory cell infiltration and histologic evidence of injury in the lung at early and late time points after i.t. LPS challenge in 4 mouse strains. In all strains, we observed lymphocyte recruitment to the alveolar com-

Conflict of interest: The authors have declared that no conflict of interest exists.
Citation for this article: *J. Clin. Invest.* **119**:2898–2913 (2009). doi:10.1172/JCI36498.

partment of the lung within several days of i.t. LPS instillation (data not shown). Because little has been described of lymphocyte participation in any aspect of ALI, we sought to examine a potential role for lymphocytes in injury and/or repair by exposing *Rag-1*$^{-/-}$ mice and WT C57BL/6 mice to i.t. LPS, followed by assessment of injury parameters at intervals to day 10. Mortality in *Rag-1*$^{-/-}$ mice was approximately 2-fold higher than the 15%–20% observed in WT mice (Figure 1A). Surviving *Rag-1*$^{-/-}$ mice continued to appear ill, with decreased activity, lack of grooming, piloerection, and sustained weight loss (Figure 1B). In contrast, WT mice exhibited return of activity and grooming by day 6 after LPS and gained weight back to baseline levels by day 10 (Figure 1B). Routine BAL fluid cultures revealed no evidence of infection in any mice.

Measures of lung injury, including BAL protein (Figure 1C), BAL total cell (Figure 1D) and differential counts (Figure 1E), and lung histology (Figure 1, F and G), indicated similar degrees of injury in the 2 groups on days 1 and 4, but striking evidence of delayed resolution in *Rag-1*$^{-/-}$ mice on day 10. BAL protein and cell counts were higher on day 10 after LPS in *Rag-1*$^{-/-}$ mice than in WT mice. Alveolar neutrophils, which peaked in both groups on day 4 (Figure 1E), were nearly absent (<1%) by day 10 in WT mice, but remained elevated in *Rag-1*$^{-/-}$ mice. BAL macrophages were also higher in *Rag-1*$^{-/-}$ mice than WT mice on day 10. In WT mice, BAL lymphocytes increased significantly by day 4 after i.t. LPS and remained elevated to day 10. Lymphocytes were absent in *Rag-1*$^{-/-}$ mice.

Histology revealed marked neutrophilic alveolar and interstitial infiltration by day 1 after LPS in WT mice, with increased interstitial thickening and mixed cellular infiltration on day 4 (Figure 1F). By day 10, histology had returned to nearly normal in WT mice. In the *Rag-1*$^{-/-}$ mice, histologic changes were similar to those in WT mice on days 1 and 4 after LPS; however, interstitial thickening and cellular infiltration persisted to day 10, indicating marked impairment of resolution. Semiquantitative histopathological lung injury scores confirmed the day-10 differences seen in the *Rag-1*$^{-/-}$ group (Figure 1G). Movat staining revealed increased interstitial collagen in both WT and *Rag-1*$^{-/-}$ mice on day 4 after i.t. LPS (Figure 1H). Interstitial collagen was markedly reduced in WT mice by day 10, but persisted in *Rag-1*$^{-/-}$ mice. In summary, multiple parameters indicate that despite early injury similar to that of WT animals, lymphocyte-deficient *Rag-1*$^{-/-}$ mice manifested a profound impairment in resolution of lung injury after i.t. LPS.

Alveolar Tregs increase after ALI. In order to begin understanding the potential contribution of specific lymphocyte subsets to the LPS response, we performed flow cytometry on lung and alveolar compartment cells to define temporal changes in lymphocyte populations. No B lymphocytes (CD45-B220) were identified in the alveolar compartment (data not shown), but we observed a progressive influx of CD3$^+$ (CD4$^+$, CD8$^+$, and CD4$^-$CD8$^-$) T lymphocytes into the alveolar compartment (Supplemental Figure 1; supplemental material available online with this article; doi:10.1172/JCI36498DS1). Lymphocytes were not increased in the lung parenchyma (Supplemental Figure 2). To begin testing potential functional roles for lymphocytes in the response, we performed adoptive transfer (AT) of cells into *Rag-1*$^{-/-}$ mice by tail vein injection 60 minutes after LPS instillation. Transfer of whole spleen cells isolated from congenic CD45.1 naive WT mice (to distinguish donor from recipient) uniformly produced complete resolution of i.t. LPS–induced lung injury in *Rag-1*$^{-/-}$ mice by day 10 (Figure 2A); injury did not resolve in mice receiving PBS sham infusion or AT of CD4-depleted spleen cells, as also confirmed by lung injury scores (Figure 2B). Flow cytometry revealed that donor congenic cells trafficked into the alveolar compartment of recipient mice. These findings indicated that CD4$^+$ cells mediate resolution of lung injury.

Recent reports demonstrate important roles for Tregs in downregulation of inflammation, best established in antigen-specific models (20–22). Given that resolution of injury in our model required CD4$^+$ cells, we hypothesized that Tregs play a critical role in this process. Flow cytometry revealed that the number of CD4$^+$CD25$^+$ cells increased in the alveolar compartment of WT mice as early as day 1 after i.t. LPS (Figure 2, C and D). The number of CD4$^+$CD25$^+$ cells did not increase in the lung tissue (data not shown).

In order to differentiate activated CD4$^+$ cells, which can induce CD25 from Tregs, we performed intracellular staining for the transcription factor Foxp3, which is the best-established marker to define murine Tregs and is necessary for the suppressive function exhibited by these cells (23). Approximately 90% of CD4$^+$CD25$^+$ cells in the spleens of control mice were Foxp3$^+$ (Figure 2C). A similar percentage of CD4$^+$CD25$^+$ cells were Foxp3$^+$ in the spleens of LPS-treated mice (data not shown). The percentage of CD4$^+$CD25$^+$ alveolar cells expressing Foxp3$^+$ was approximately 60% at day 1 after i.t. LPS, fell to 38% by day 4, and increased to about 80% by day 10, nearing the frequency for Foxp3$^+$ expression in spleen cells and similar to the frequency usually reported for mice (13). We believe this difference in Foxp3 expression between alveolar and spleen cells reflects both an increase in CD25 expression in non-Tregs (activated T cells) and downregulation of Foxp3 by inflammation and/or LPS, as recently described (24) and further evaluated below. The absolute number of alveolar CD4$^+$CD25$^+$Foxp3$^+$ cells increased significantly by day 1 after i.t. LPS, peaked at day 7, and remained elevated at day 10 (Figure 2D). To reinforce that these cells were Tregs, we also examined expression of a surface marker, Folate receptor 4 (FR4), recently found to be highly expressed in both naturally occurring and TGF-β–induced Tregs (25). Greater than 90% of CD4$^+$CD25$^+$ cells in mouse spleen expressed FR4 (Figure 2E), similar to what we observed for Foxp3. After i.t. LPS, changes in the percentage of FR4$^+$ cells over time were similar to the profile for Foxp3. Figure 2F summarizes the dynamic changes in alveolar Treg abundance; these observations indicate that Tregs progressively increase in the alveolar compartment in the transition from injury to resolution.

When examining the colabeling of Tregs for Foxp3$^+$ and FR4$^+$ expression, we noted that there was a tight correlation between both markers in splenic Tregs. Greater than 98% of Foxp3$^+$ spleen Tregs colabeled with FR4$^+$, while more than 90% of CD4$^+$CD25$^+$FR4$^+$ spleen cells expressed Foxp3$^+$. This correlation was similar in alveolar CD4$^+$CD25$^+$ cells except at the peak of injury at day 4 after i.t. LPS, when approximately 60% of Foxp3$^+$ cells colabeled for FR4$^+$, whereas about 40% of CD4$^+$CD25$^+$FR4$^+$ alveolar cells coexpressed Foxp3$^+$ (Supplemental Figure 3).

Transfer of Tregs mediates resolution of ALI in lymphopenic mice. In order to specifically assess a potential role for Tregs in mediating resolution of lung injury, we isolated CD4$^+$CD25$^-$ or CD4$^+$CD25$^+$ cells from spleens of congenic CD45.1 WT mice and performed AT into *Rag-1*$^{-/-}$ mice 1 hour after instillation of i.t. LPS. Approximately 90% of CD4$^+$CD25$^+$ spleen cells were Foxp3$^+$ at the time of transfer. Donor lymphocytes (CD45.1) were detected in the BAL of *Rag-1*$^{-/-}$ mice after LPS, but were not detected in the BAL of uninjured control *Rag-1*$^{-/-}$ mice (data not shown), which revealed that Tregs traveled into the inflamed environment. Transfer of

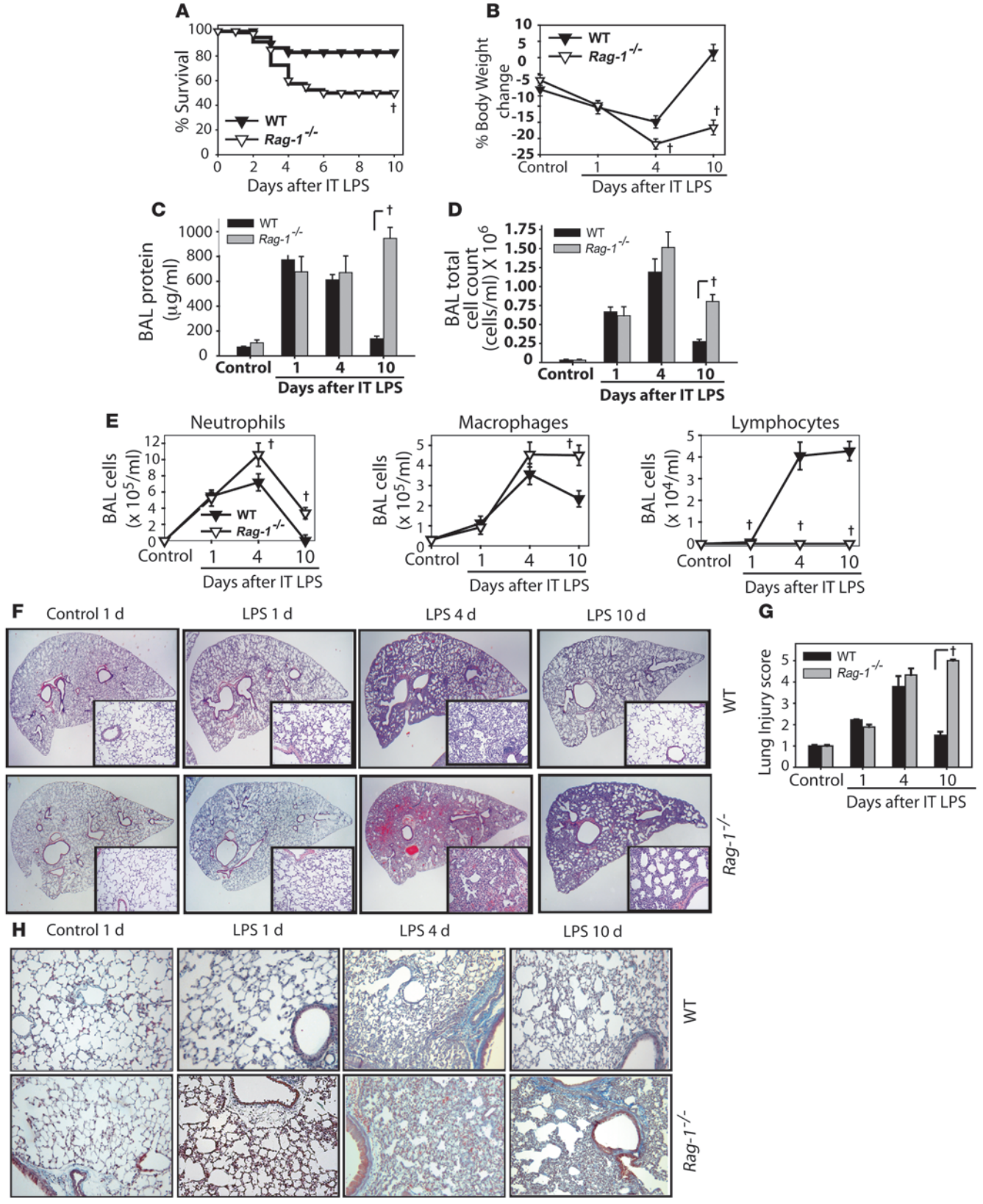
A
% Survival
Days after IT LPS
WT
Rag-1 -/-
B
% Body Weight change
Control
Days after IT LPS
C
BAL protein (μg/ml)
D
BAL total cell count (cells/ml) X 10^6
E
Neutrophils
Macrophages
Lymphocytes
BAL cells (x 10^5/ml)
BAL cells (x 10^4/ml)
F
Control 1 d
LPS 1 d
LPS 4 d
LPS 10 d
G
Lung Injury score
H

Figure 1
Resolution of lung injury is markedly impaired in lymphocyte-deficient *Rag-1*$^{-/-}$ mice. Mice (n = 8–10 per group per time point) were challenged with i.t. LPS. (**A** and **B**) Survival (**A**) and body weight relative to baseline (**B**) were plotted after injury. (**C**–**E**) BAL total protein (**C**), total cell counts (**D**), and differential cell counts (**E**) were determined in WT and *Rag-1*$^{-/-}$ mice after treatment with water control or with LPS. (**F**) Lung sections were stained with H&E. Original magnification, ×20; ×100 (insets). (**G**) Histopathological mean lung injury scores from ×20 lung sections (n = 5 animals per group per time point). (**H**) Movat stain for collagen (blue) from WT and *Rag-1*$^{-/-}$ mice after injury. Original magnification, ×40. $^{\dagger}P < 0.05$, log-rank test (mortality curves) and unpaired Student's t test (other injury parameters).

Tregs significantly improved survival, in contrast to the effects of saline control infusion or AT of CD4-depleted spleen cells or CD4$^+$CD25$^-$ cells (Figure 3A). Surviving mice treated with PBS or CD4$^+$CD25$^-$ cells appeared ill through day 10, whereas mice receiving Tregs had return of activity and grooming (generally by day 6) as well as weight gain back to baseline by day 10 (data not shown). Because the profile for numerous endpoints was similar between WT and *Rag-1*$^{-/-}$ mice on days 1 and 4 after LPS (Figure 1), we examined day-10 injury parameters to assess the effectiveness of AT to promote resolution. LPS-treated mice receiving PBS or CD4$^+$CD25$^-$ cells had impaired injury resolution, with persistent histologic changes (Figure 3, B and C), as well as elevation of BAL protein (Figure 3D) and cell counts (Figure 3E) on day 10. Similarly, lung injury did not resolve in *Rag-1*$^{-/-}$ mice receiving isolated CD8$^+$ cells. In contrast, mice receiving Tregs exhibited nearly complete resolution of each of these parameters. Although transfer of 10^6 Tregs produced injury resolution, transfer of 10^4 or 10^5 Tregs did not produce resolution (data not shown). Resolution of lung injury was achieved even when we transferred Tregs into *Rag-1*$^{-/-}$ mice as late as 24 hours after i.t. LPS, as evidenced by lung histology (Figure 3F) and by decreased BAL total cells and protein (data not shown), a striking finding that suggests a potential role as rescue therapy in ALI.

Phenotype and function of alveolar Tregs during resolution of ALI. We sought to better define both the phenotypic changes and the function of Tregs recruited into the alveolar compartment after i.t. LPS. As described above, the percentage of alveolar CD4$^+$CD25$^+$ cells in LPS-treated WT mice that expressed Foxp3 (or FR4) was reduced compared with the percentages observed in spleen. Indeed, when we performed AT of isolated CD4$^+$CD25$^+$ cells from WT spleen that were greater than 90% Foxp3$^+$ into *Rag-1*$^{-/-}$ mice, the percentage of Foxp3$^+$ cells in BAL on day 4 after LPS fell below 35% before returning nearly to baseline levels by day 10 (Figure 4A), similar to the pattern observed in WT mice. A recent report indicates that LPS can downregulate Foxp3 expression (21). To determine whether LPS could alter Foxp3 expression in isolated CD4$^+$CD25$^+$ cells, we purified Tregs from spleens of WT mice (85%–90% CD4$^+$CD25$^+$Foxp3$^+$) and placed them in culture in the presence or absence of LPS and in the presence or absence of macrophages (Figure 4, B and C). Challenge of isolated Tregs with LPS for 24 hours had little effect on the expression of Foxp3 and FR4 in the purified Treg population (Figure 4, B and C). Similarly, the addition of macrophages had only a modest effect on Foxp3 and FR4 expression. In contrast, the incubation of Tregs with macrophages and LPS for only 24 hours resulted in a significant decrease in both Foxp3 and FR4 expression (Figure 4C). This finding suggests that both Foxp3 and FR4 expression in Tregs may be downregulated in the inflammatory alveolar microenvironment.

Tregs were originally described as suppressing the proliferation of other lymphocyte subsets (26). We sought to determine whether CD4$^+$CD25$^+$ cells in the alveolar compartment could suppress proliferation of responder lymphocytes. We performed fluorescence-activated cell sorting (FACS) to isolate CD4$^+$CD25$^+$ cells from the BAL of WT mice on day 4 after i.t. LPS. In these experiments, approximately 50% of the CD4$^+$CD25$^+$ cells isolated from BAL were Foxp3$^+$. When responder CD4$^+$CD25$^-$ cells (harvested from WT spleen) were incubated with anti-CD3 antibodies and irradiated APCs, proliferation (as assessed by ^{3}H thymidine uptake) increased approximately 15-fold (Figure 4D). Coculture of CD4$^+$CD25$^-$ responder cells with CD4$^+$CD25$^+$ cells isolated from spleen (>90% Foxp3$^+$) significantly reduced proliferation of stimulated responder cells. When CD4$^+$CD25$^+$ cells isolated from BAL of LPS-injured mice were cocultured with anti-CD3– and APC–stimulated responder cells, responder cell proliferation was reduced, comparable to the reduction produced by coculture with spleen Tregs.

Together, the results of these studies indicate that Foxp3 and FR4 downregulation in Tregs occurs when LPS-activated macrophages are present. This likely contributes to the reduction in the percentage of alveolar CD4$^+$CD25$^+$ cells that are Foxp3$^+$ in vivo after LPS, as we observed in both WT and *Rag-1*$^{-/-}$ mice. In addition, CD4$^+$CD25$^+$ cells recruited to the alveolar compartment manifest suppressive function, as classically described for Tregs.

Manipulation of Tregs in WT mice determines resolution of lung injury. Given that AT of Tregs restored resolution of lung injury in *Rag-1*$^{-/-}$ mice, we determined whether Tregs participate in the response to LPS in WT mice. Administration i.p. of mAb PC61 against CD25 (27, 28) produced a greater than 90% reduction in CD4$^+$CD25$^+$ cells in spleen and blood (data not shown). WT mice receiving PC61 had reduced survival after LPS compared with isotype Ab–treated mice (Figure 5A), as well as higher BAL protein (Figure 5B) and cell counts (Figure 5C). Lung histology and lung injury scores revealed a delay in resolution in the Treg-depleted group (Figure 5, D and E), demonstrating a fundamental role for endogenous Tregs in resolution of ALI in normal hosts.

To examine the possibility that increasing the number of Tregs in WT mice could improve survival and/or accelerate resolution in response to higher doses of LPS, we adoptively transferred Tregs into WT mice following administration of twice our standard dose of LPS. Of the PBS-infused mice, 4 of 10 died, whereas only 1 of 10 mice receiving Tregs died (Figure 5F). Consistent with the effect on survival, lung histology revealed accelerated resolution of injury in Treg-infused mice compared with controls (Figure 5G), and surviving Treg-treated mice were clinically improved (e.g., grooming, activity, and weight gain) compared with controls. In addition, BAL protein and cell counts (data not shown) were significantly reduced in the Treg-treated group. These studies indicate that in addition to mediating resolution of ALI in *Rag-1*$^{-/-}$ mice, Tregs play a central role in resolution of lung injury in WT mice.

Tregs alter the alveolar inflammatory milieu. We examined the abundance of pro- and antiinflammatory cytokines in the alveolar compartment, as this balance is likely to play an important role in determining the course of the LPS response. Proinflammatory cytokines TNF-α and IL-6 peaked at day 1 in both WT and *Rag-1*$^{-/-}$ mice, but were higher in *Rag-1*$^{-/-}$ mice on days 4 and 10 (Figure 6A). AT of Tregs, but not CD4$^+$CD25$^-$ cells, into *Rag-1*$^{-/-}$ mice reduced TNF-α

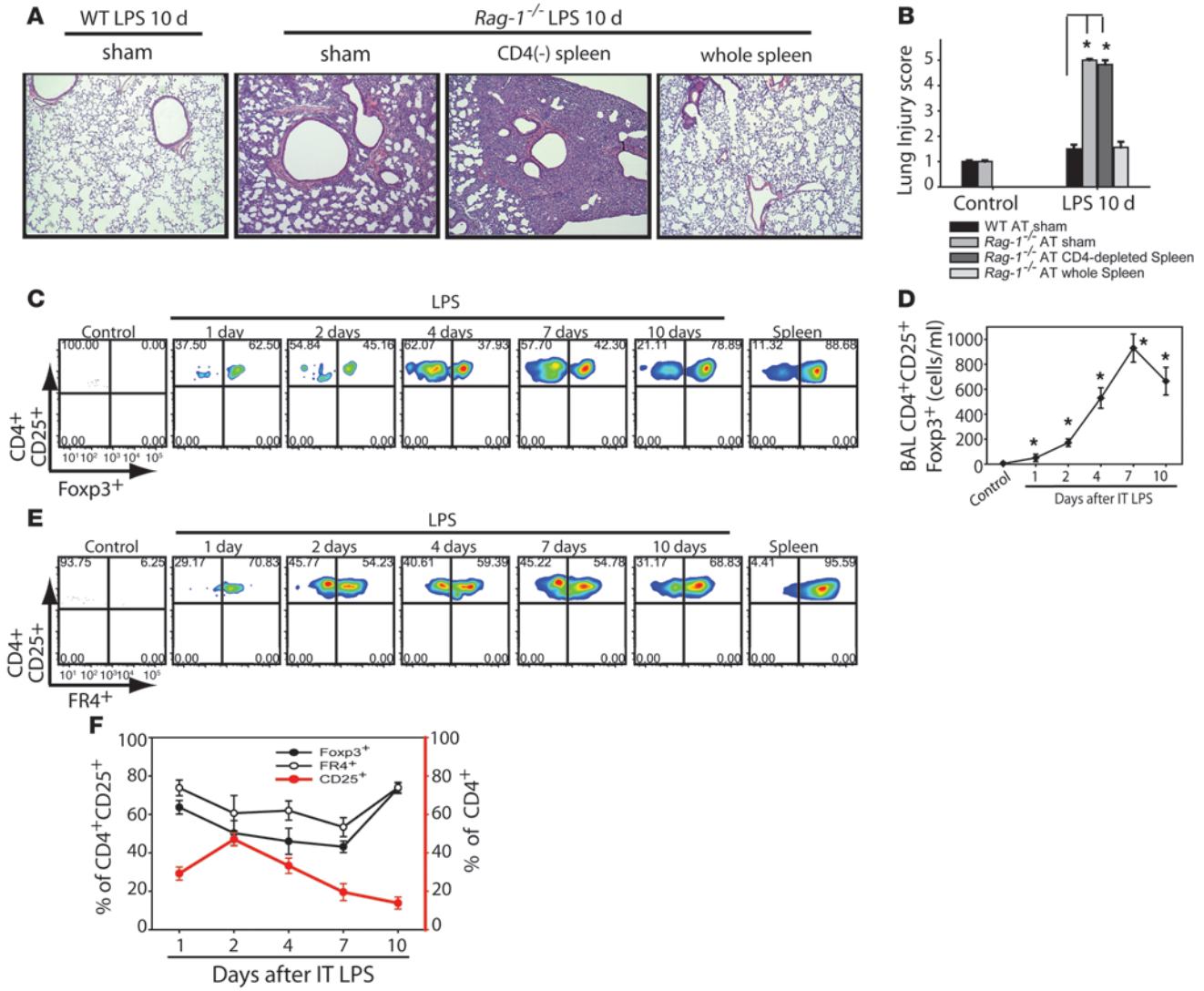

Figure 2

Alveolar CD4⁺CD25⁺Foxp3⁺ Tregs increase after injury with i.t. LPS. (**A**) Representative lung sections were stained with H&E (n = 10 per group) to reveal morphologic changes on day 10 after i.t. LPS in *Rag-1*$^{-/-}$ mice. Animals received AT via tail vein injection of PBS sham treatment, 10 × 10^6 WT CD4-depleted splenocytes, or WT splenocytes from whole spleen. Original magnification, ×40. (**B**) Mean histopathological lung injury scores by day 10 after i.t. LPS (n = 6–8 animals per group). (**C**) BAL cells from WT animals were analyzed by flow cytometry for the presence of CD4⁺CD25⁺ surface staining and intracellular transcription factor Foxp3⁺ at baseline and after injury; corresponding populations in the spleen were used for comparison. (**D**) Absolute Treg numbers at baseline and after injury. *P < 0.05 versus control. (**E**) Surface staining for FR4 was determined in CD4⁺CD25⁺ cells from spleen and BAL after LPS. (**F**) Relative expression of Foxp3 and FR4 in CD4⁺CD25⁺ cells (left axis), as well as CD25⁺ expression in the CD4⁺ pool (right axis), isolated from the BAL at baseline and after i.t. LPS. Numbers within plots in **C** and **E** denote the percentage of cells in the respective quadrants.

and IL-6 to WT levels. A similar profile (higher in *Rag-1*$^{-/-}$ mice, and reduced by AT of Tregs) was observed for IL-12p40 on day 10, but not at earlier times. IL-10 was not detected in the BAL fluid. The reparative cytokine TGF-β was significantly increased in WT mice, but not *Rag-1*$^{-/-}$ mice, on day 4 after LPS. Transfer of Tregs into *Rag-1*$^{-/-}$ mice produced a doubling of TGF-β on day 4 after LPS, while AT of CD4⁺CD25⁻ cells did not alter the TGF-β profile. The lymphocyte chemokine RANTES increased in both WT and *Rag-1*$^{-/-}$ mice on day 1, but was lower in WT and Treg-treated *Rag-1*$^{-/-}$ mice on days 4 and 10. Myocyte chemoattractant protein–1 (MCP-1) was increased in *Rag-1*$^{-/-}$ mice (consistent with the observed increase in alveolar macrophages; Figure 1F) and was reduced by AT of Tregs. BAL IFN-γ increased similarly in both WT and *Rag-1*$^{-/-}$ mice, and IL-4 and IL-13 were not significantly elevated in either group (data not shown), consistent with a polarized type 1 response after LPS-induced lung injury. The general pattern of alveolar cytokine/chemokine expression in Treg-depleted WT mice on day 4 after i.t. LPS (Figure 6B) was similar to that in *Rag-1*$^{-/-}$ mice, reinforcing a central role for Tregs in modulating the alveolar inflammatory milieu.

Alveolar macrophages are thought to play a prominent role in the pathogenesis of lung injury (29, 30), and they constituted greater than 80% of the non-neutrophil alveolar cells on days 4 and 10 after

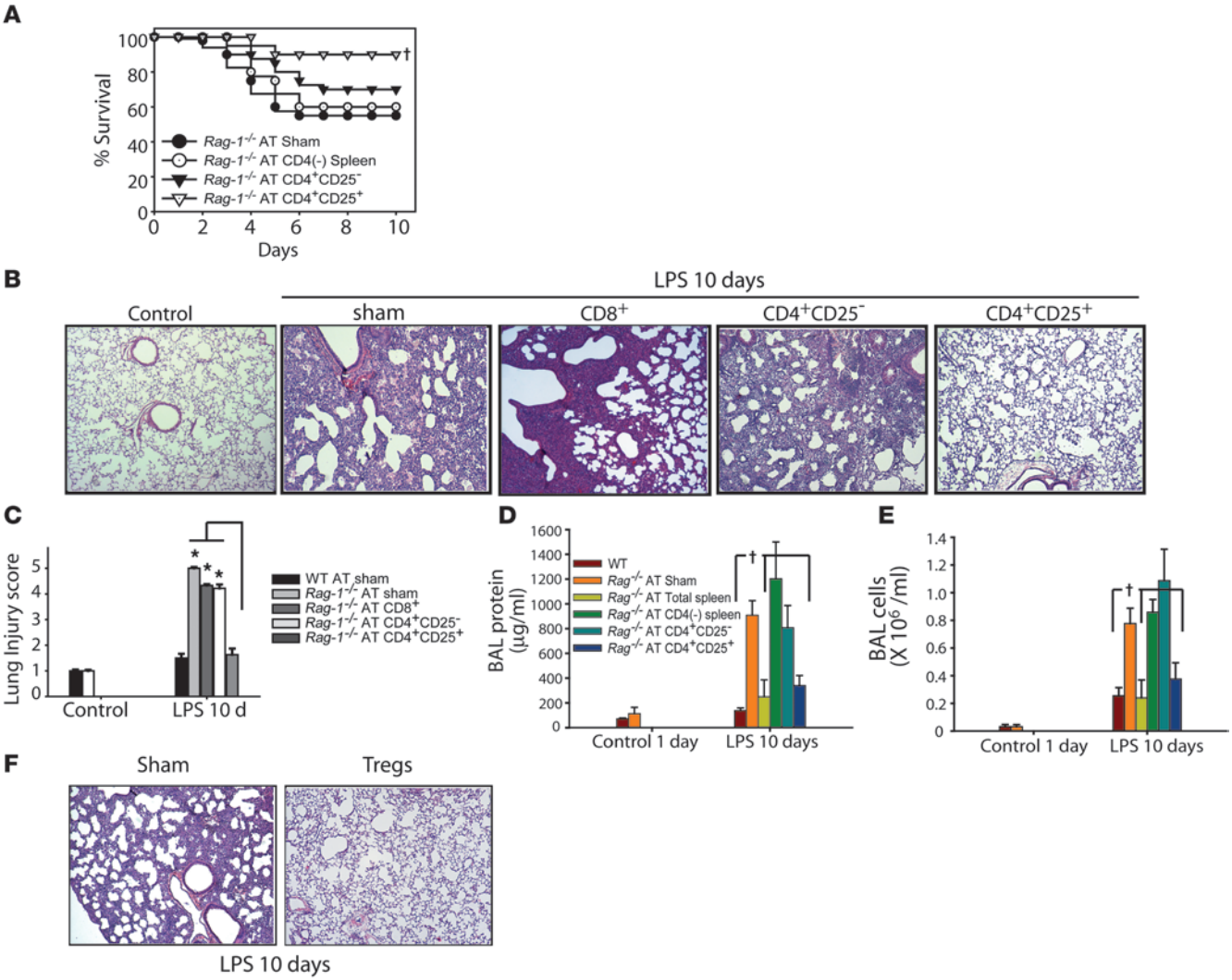

Figure 3

AT of Tregs mediates resolution of lung injury in *Rag-1*$^{-/-}$ mice. *Rag-1*$^{-/-}$ mice were challenged with i.t. LPS and 1 hour afterward received PBS sham treatment or 1.0 × 10^6 WT CD4$^+$CD25$^-$ or WT CD4$^+$CD25$^+$ splenocytes. (**A**) *Rag-1*$^{-/-}$ mouse survival over a 10-day period. $^\dagger P < 0.05$ versus sham control, log-rank test. (**B**) H&E stain of representative lung sections on day 10 after i.t. LPS and infusion of PBS or the indicated lymphocyte subsets. Original magnification, ×40. (**C**) Mean histopathological lung injury scores (n = 8–10 animals per group). $^*P < 0.05$. (**D** and **E**) BAL total protein (**D**) and total cell counts (**E**) were determined in WT and *Rag-1*$^{-/-}$ mice on day 10 after AT (n = 10 per group). $^\dagger P < 0.05$ versus *Rag-1*$^{-/-}$ sham control. (**F**) Lung H&E staining demonstrate that AT of Tregs into injured *Rag-1*$^{-/-}$ mice as late as 24 hours after i.t. LPS achieved resolution of lung injury (n = 5 per group). Original magnification, ×40.

LPS, as assessed by cytospins and flow cytometry (F4/80 labeling). To determine whether Tregs can directly alter macrophage function, we cocultured CD4$^+$CD25$^+$ and CD4$^+$CD25$^-$ cells with alveolar macrophages isolated from LPS-naive WT mice. LPS stimulated a 20-fold increase in TNF-α in the macrophage supernatant at 24 hours (Figure 6C). Addition of CD4$^+$CD25$^+$ cells (approximately 90% Foxp3$^+$), but not CD4$^+$CD25$^-$ cells, 2 hours after LPS significantly attenuated TNF-α production, even at lymphocyte/macrophage ratios as low as 1:10, which indicates that Tregs can alter alveolar macrophage function to attenuate components of the innate immune response. Treg-mediated effects have been described as being both contact dependent and contact independent. To examine the contact requirement for Treg-mediated downregulation of macrophage TNF-α production, we performed coculture studies in a 96-well Transwell system. Isolated macrophages from LPS-naive WT mice were plated in the bottom well and stimulated with LPS. At 2 hours after LPS exposure, spleen CD4$^+$CD25$^+$ cells or CD4$^+$CD25$^-$ cells were added into either the bottom or the top well at a lymphocyte/macrophage ratio of 1:2 (Figure 6D). When added to the bottom well, Tregs (but not CD4$^+$CD25$^-$ cells) reduced LPS-stimulated macrophage TNF-α production by greater than 60%. When lymphocytes were added to the top well, TNF-α production was not significantly reduced, even when 4 times as many Tregs were added to the top well (data not shown). Addition of 50 mg/ml anti–TGF-β inhibited the direct response, but not the indirect response (Figure 6D).

To determine whether Tregs also enhance the antiinflammatory response of macrophages, we examined potential regulation of macrophage TGF-β secretion by Tregs. It has previously been shown

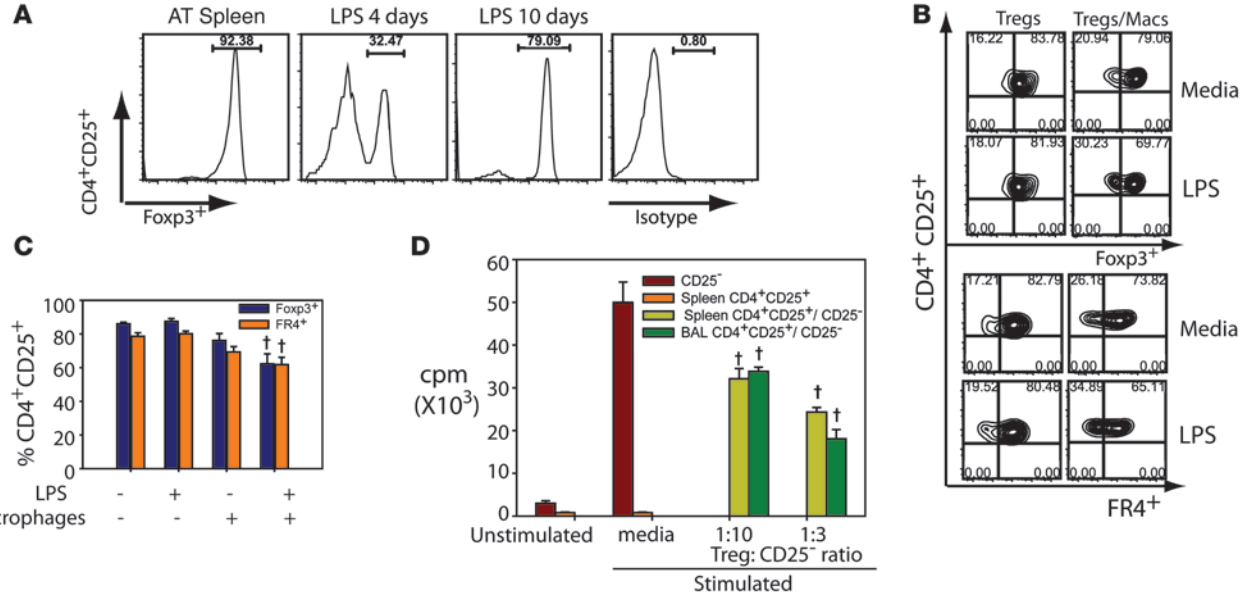

Figure 4

Phenotype and function of alveolar Tregs during resolution of ALI. (**A**) Histograms showing the percentage of Foxp3+ cells in the pool of donor CD4+CD25+ splenocytes (AT spleen) as well as in CD4+CD25+ cells recovered in the BAL from LPS-injured *Rag-1*$^{-/-}$ mice on days 4 and 10 after LPS. Labeling for isotype control Ab at day 10 is also shown. (**B**) Purified Tregs from naive WT spleens were cultured in the presence or absence of 100 ng/ml LPS and/or macrophages. Representative flow cytometry shows the relationship between Foxp3 and FR4 expression under different conditions. Numbers within plots denote the percentage of cells in the respective quadrants. (**C**) Relative expression of Foxp3 and FR4 in CD4+CD25+ cells from the experiments in **B**. †$P < 0.05$ versus Tregs without LPS or macrophages. (**D**) Proliferative responses of CD4+CD25− lymphocytes to 0.5 mg/ml anti-CD3 and irradiated APCs (Stimulated) in the presence or absence of CD4+CD25+ cells isolated from spleen or sorted from BAL of WT mice on day 4 after LPS and cultured at the indicated ratios. Unstimulated CD4+CD25− lymphocytes were not exposed to anti-CD3 and irradiated APCs. †$P < 0.05$ versus media-stimulated CD25− cells.

that alveolar macrophages cannot be stimulated by LPS in vitro to make TGF-β (31, 32); our own experience was similar. In order to examine potential effects of Tregs on macrophage TGF-β production, we used thioglycollate-induced peritoneal macrophages and exposed them to LPS in vitro. Active TGF-β was detected in the supernatant (Figure 6E). Coincubation of thioglycollate-induced macrophages with Tregs and LPS increased TGF-β secretion 2.5-fold; coincubation with CD4+CD25− cells had no effect.

No TGF-β secretion was detected in the supernatants of isolated LPS-stimulated Tregs, nor could we detect Treg cell surface expression of latency-associated peptide (LAP; Figure 6F), a reported marker for TGF-β–mediated Treg suppressive effects (33). We also did not detect LAP in ex vivo BAL CD4+CD25+ cells from LPS-stimulated mice or in CD4+CD25+ cells cocultured under basal conditions or after LPS stimulation in the presence or absence of macrophages (data not shown). In contrast, we detected Treg cell surface LAP in a positive control experiment in which CD4+CD25+ splenocytes were stimulated with anti-CD3 (10 μg/ml) and IL-2 (50 U/ml) for 4 days (Figure 6F), as previously reported (33). These findings not only indicate that Tregs are not the source of increased TGF-β in response to LPS, they are consistent with contact-dependent Treg-mediated downregulation of macrophage proinflammatory responses as well as with Treg-enhanced production of TGF-β by activated macrophages.

Tregs enhance alveolar neutrophil clearance. Persistence of alveolar neutrophils in ALI patients is associated with worse outcomes (34, 35). In our studies, we observed a significant difference in alveolar neutrophils between WT and *Rag-1*$^{-/-}$ mice (Figure 7A), as well as between Treg-depleted and WT mice (Figure 7B). Multiple mechanisms may contribute to both the increase and persistence of neutrophils in *Rag-1*$^{-/-}$ mice, including enhanced recruitment. However, the expression of keratinocyte chemokine (KC), G-CSF, and GM-CSF, 3 potent neutrophil chemokines/survival factors in BAL fluid, varied between WT and *Rag-1*$^{-/-}$ mice on day 1, but was not different on subsequent days (Supplemental Figure 4). In contrast, BAL neutrophil apoptosis on day 4 after LPS was reduced in *Rag-1*$^{-/-}$ mice, and increased after AT of Tregs, but not after transfer of CD4+CD25− cells (Figure 7C).

We also observed a similar effect of Tregs on neutrophil apoptosis in ex vivo cultures. Mixed cultures of neutrophils and macrophages, isolated from BAL of *Rag-1*$^{-/-}$ mice on day 4 after i.t. LPS, were incubated for 24 hours with medium alone, CD8+cells, CD4+CD25− cells, or CD4+CD25+ cells (90% Foxp3+) isolated from WT spleen. Both neutrophil apoptosis (Figure 7D) and macrophage-mediated efferocytosis (Figure 7E) were significantly increased in the presence of Tregs. Furthermore, the fraction of neutrophils persisting in macrophage-neutrophil cocultures from WT and *Rag-1*$^{-/-}$ mice at 24 and 48 hours was reduced when Tregs were present compared with cocultures in the absence of Tregs (Supplemental Figure 5). Together with the in vivo results from LPS-treated mice, these studies indicate that Tregs play a critical role in apoptosis and clearance of neutrophils from the alveolar compartment after lung injury.

Treg-mediated resolution is abrogated by interference with TGF-β, not IL-10. The suppressive effects of Tregs have been proposed to be mediated by IL-10 or TGF-β in different models of inflammation

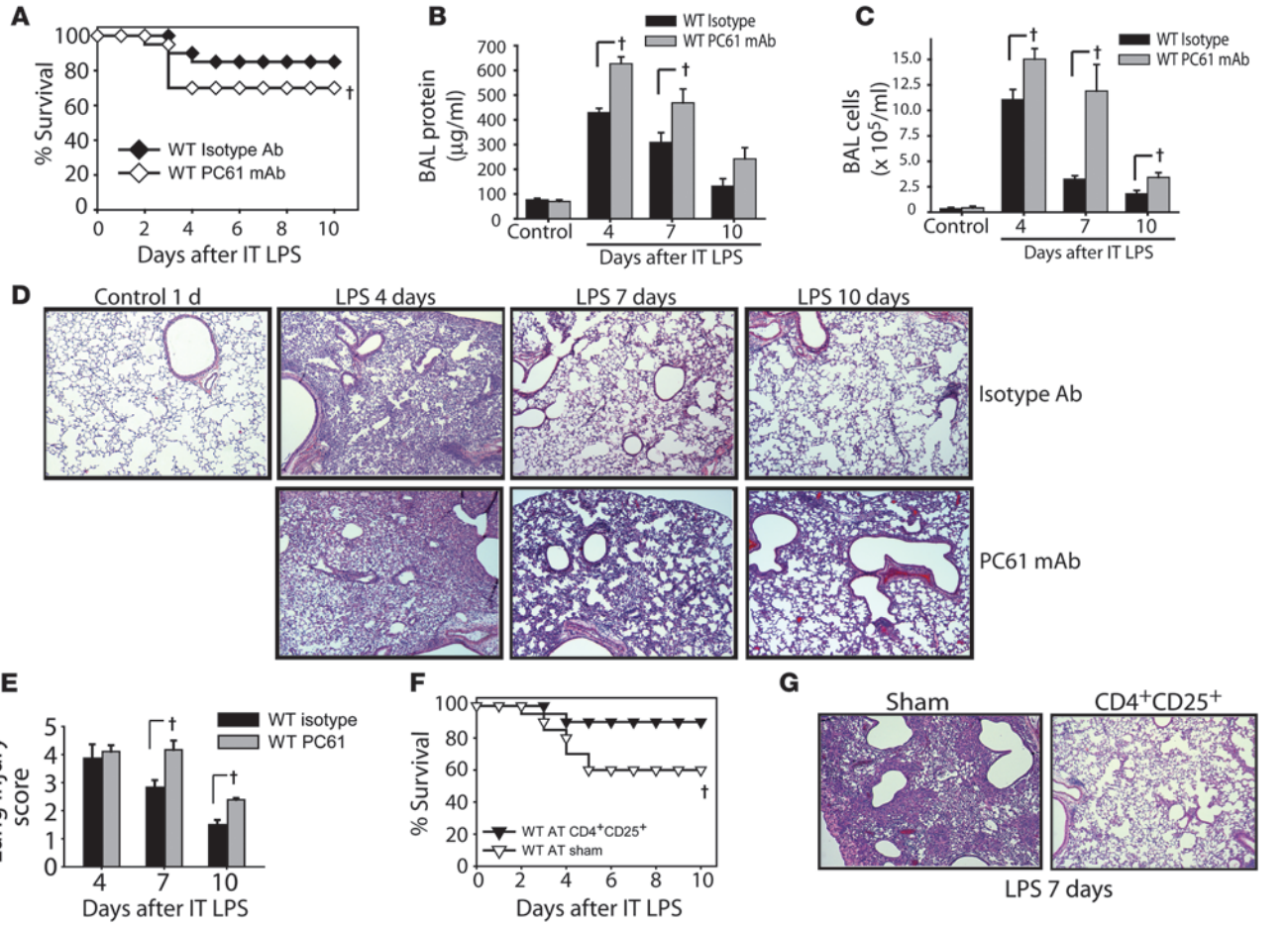

Figure 5

Manipulation of Tregs in WT mice determines resolution of lung injury. WT mice were pretreated with 0.5 mg of CD25-depleting PC61 mAb or isotype Ab i.p. on days –2, 0, 3, and 6 relative to i.t. LPS (day 0). (**A**) Survival curves over 10 days ($n = 20$ per group). (**B** and **C**) BAL total protein (**B**) and total cell counts (**C**) were determined at the indicated time points ($n = 6$ per group per time point). (**D**) H&E stain of representative lung sections at the indicated times. Original magnification, ×40. (**E**) Mean lung injury scores ($n = 4$ per group per time point). (**F**) To assess the effect of increasing Treg number, WT mice were challenged with twice our standard i.t. LPS dose (7.5 mg/kg) and 1 hour later given an infusion of 2×10^6 Tregs or 100 μl PBS sham treatment, and survival was assessed ($n = 10$ per group). (**G**) Representative H&E-stained lung sections on day 7 after LPS in mice receiving PBS or Tregs. Original magnification, ×40. †$P < 0.05$ versus respective control, log-rank test (mortality curves) and unpaired Student's *t* test (other parameters).

(33, 36, 37). To examine potential roles for these molecules in our model of Treg-dependent resolution of lung injury, we compared the response to LPS in *Rag-1*$^{-/-}$ mice after AT of *IL-10*$^{-/-}$ Tregs (harvested from the spleens of *IL-10*$^{-/-}$ mice) or after AT of WT Tregs followed by treatment with an anti–TGF-β Ab or isotype Ab (Figure 8A). On day 7 after LPS, PBS-treated *Rag-1*$^{-/-}$ mice exhibited persistence of inflammation in the lung. *Rag-1*$^{-/-}$ mice receiving *IL-10*$^{-/-}$ Tregs had near-complete resolution of injury by day 7. Similarly, *Rag-1*$^{-/-}$ mice that received WT Tregs followed by isotype Ab also exhibited near-complete resolution of lung injury. In contrast, *Rag-1*$^{-/-}$ mice that received WT Tregs followed by anti–TGF-β Ab had impaired resolution of lung injury, as assessed by lung histology and lung injury scores (Figure 8, A and B), as well as persistent elevation of BAL protein (Figure 8C) and cell counts (Figure 8D). BAL neutrophils were 3-fold greater in the group that received anti–TGF-β compared with PBS- or isotype Ab–treated mice (Figure 8D). Flow cytometry with Annexin V/7-AAD staining revealed that neutrophil apoptosis decreased in the group receiving anti–TGF-β Ab compared with isotype Ab–treated mice (Figure 8E), indicating a potential mechanism by which inhibition of TGF-β signaling contributes to delayed resolution of lung injury. Although resolution was delayed with TGF-β inhibition, all Treg-treated *Rag-1*$^{-/-}$ mice receiving anti–TGF-β survived, similar to Treg-treated *Rag-1*$^{-/-}$ mice that received isotype Ab. In marked contrast, 30% mortality was seen in PBS-treated *Rag-1*$^{-/-}$ mice.

To further examine the role of TGF-β in resolution of ALI, we inhibited TGF-β in WT mice by administering anti–TGF-β antibodies i.p. on days 0, 2, and 4 after i.t. LPS. In the anti–TGF-β group, 2 of 6 mice died on day 4, whereas all mice survived in the isotype Ab–treated group. In mice receiving anti–TGF-β antibodies, lung histology revealed delayed resolution (Figure 8F), although the differences in lung injury scores (Figure 8G) did not reach statistical significance ($P = 0.1$). Consistent with the increased mortality, BAL total cell counts and BAL neutrophils (Figure 8H) were increased in the anti–TGF-β group. BAL neutrophil apoptosis was also significantly decreased in the anti–TGF-β group (Figure 8, I and J), con-

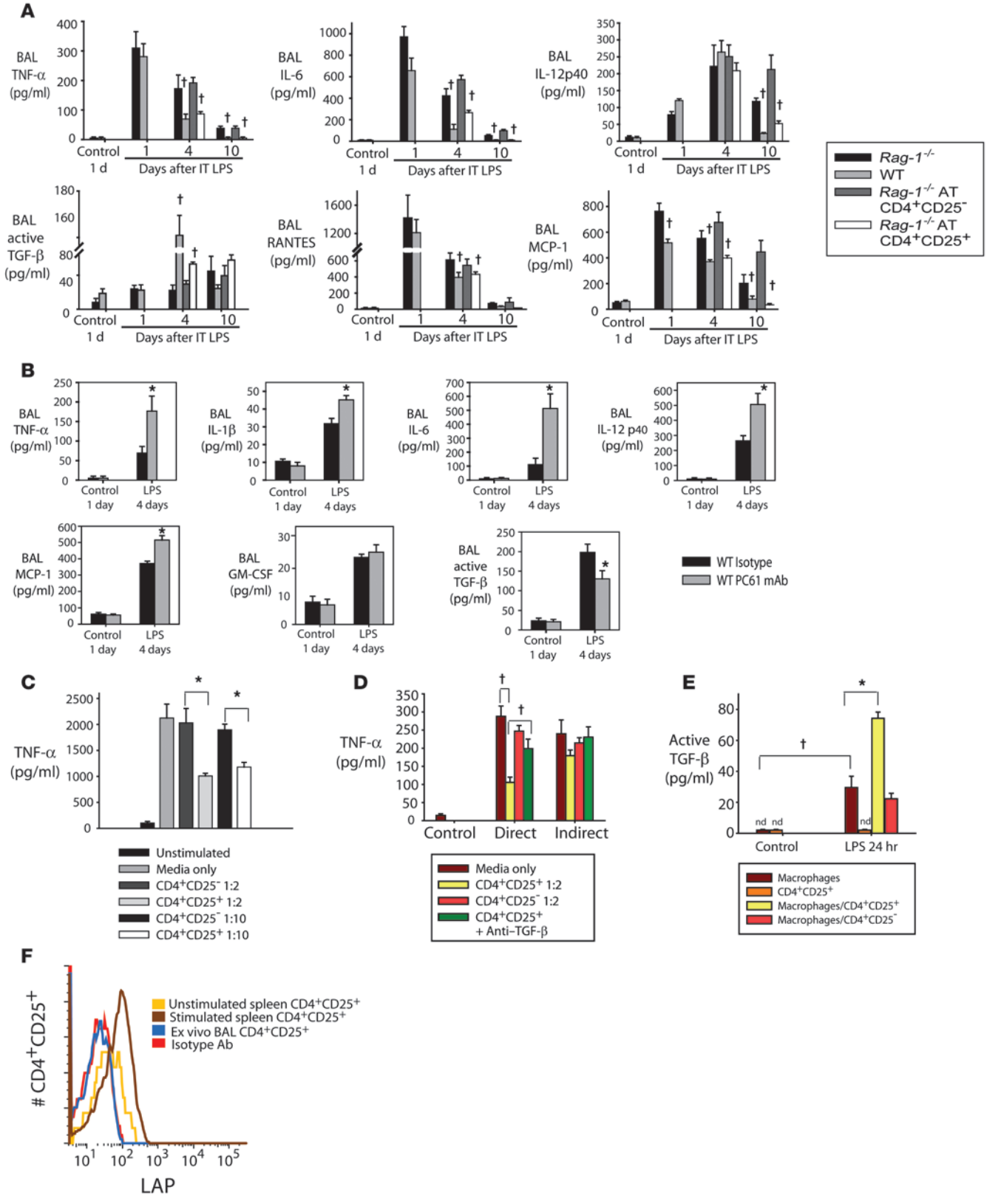
A
BAL TNF-α (pg/ml)
BAL IL-6 (pg/ml)
BAL IL-12p40 (pg/ml)
BAL active TGF-β (pg/ml)
BAL RANTES (pg/ml)
BAL MCP-1 (pg/ml)
Control 1 d
Days after IT LPS
Rag-1-/-
WT
Rag-1-/- AT CD4+CD25-
Rag-1-/- AT CD4+CD25+
B
BAL TNF-α (pg/ml)
BAL IL-1β (pg/ml)
BAL IL-6 (pg/ml)
BAL IL-12 p40 (pg/ml)
BAL MCP-1 (pg/ml)
BAL GM-CSF (pg/ml)
BAL active TGF-β (pg/ml)
Control 1 day
LPS 4 days
WT Isotype
WT PC61 mAb
C
TNF-α (pg/ml)
Unstimulated
Media only
CD4+CD25- 1:2
CD4+CD25+ 1:2
CD4+CD25- 1:10
CD4+CD25+ 1:10
D
TNF-α (pg/ml)
Control
Direct
Indirect
Media only
CD4+CD25+ 1:2
CD4+CD25- 1:2
CD4+CD25+ + Anti-TGF-β
E
Active TGF-β (pg/ml)
nd
Control
LPS 24 hr
Macrophages
CD4+CD25+
Macrophages/CD4+CD25+
Macrophages/CD4+CD25-
F
CD4+CD25+
LAP
Unstimulated spleen CD4+CD25+
Stimulated spleen CD4+CD25+
Ex vivo BAL CD4+CD25+
Isotype Ab

Figure 6
Tregs alter alveolar cytokine profiles after LPS-induced lung injury. WT and *Rag-1*$^{-/-}$ mice received LPS or sterile water as control i.t. (**A**) *Rag-1*$^{-/-}$ mice received CD4$^+$CD25$^-$ or CD4$^+$CD25$^+$ cells by tail vein injection 1 hour after LPS. BAL was harvested at the indicated times and assayed for the indicated cytokines. $^\dagger P < 0.05$ versus respective *Rag-1*$^{-/-}$ value. (**B**) BAL cytokines were assessed on day 4 after i.t. LPS in mice receiving isotype Ab or PC61. $^*P < 0.05$ versus respective isotype value. (**C**) Primary alveolar macrophages were isolated from unstimulated WT mice and exposed to 10 ng/ml LPS. (**D**) Cocultures of alveolar macrophages and the indicated T cells (1:2 lymphocyte/macrophage ratio) was performed both directly (in the bottom chamber of a Transwell plate) and indirectly (macrophages and T cells in the bottom and top chambers, respectively), and TNF-α was measured 24 hours after LPS stimulation. (**E**) Thioglycollate-induced peritoneal macrophages were harvested, plated on 24-well plates (1×10^6 cells/well), and cocultured with CD4$^+$CD25$^+$ or CD4$^+$CD25$^-$ cells or with media alone at a 1:2 lymphocyte/macrophage ratio in the presence or absence of 10 ng/ml LPS. Active TGF-β was measured in supernatants by ELISA. (**C**–**E**) $^\dagger P < 0.05$; $^*P < 0.05$. (**F**) Cell surface expression of LAP in CD4$^+$CD25$^+$ splenocytes incubated with medium (unstimulated) or cultured with 10 μg/ml anti-CD3 and 50 U/ml IL-2 (stimulated), ex vivo BAL CD4$^+$CD25$^+$ cells on day 4 after i.t. LPS, and isotype Ab control.

sistent with findings for TGF-β blockade in LPS-injured *Rag-1*$^{-/-}$ mice (Figure 7C). Moreover, addition of anti–TGF-β antibodies to in vitro macrophage-Treg cocultures (Figure 6D) abrogated Treg-mediated inhibition of macrophage TNF-α production after LPS exposure. Because WT mice exhibited a significant peak in BAL TGF-β on day 4 after i.t. LPS that was not present in *Rag-1*$^{-/-}$ mice (Figure 6A), we administered recombinant TGF-β i.p. (1 μg/mouse/dose) into injured *Rag-1*$^{-/-}$ mice on days 3 and 4 after i.t. LPS; however, this did not enhance resolution, underscoring the critical requirement for Tregs to mediate resolution.

Alveolar Tregs are present in humans with ALI. We sought to determine whether Tregs can be detected in humans with ALI. Patients were enrolled within 6 days of ALI onset, and mini-BAL (38) and blood sampling were performed on days 0, 1, and 2 after enrollment. Patient 1 was a 50-year-old woman who developed lithium toxicity complicated by acute renal failure and encephalopathy, with subsequent aspiration and development of ALI. She was enrolled within 1 day of the onset of ALI. Her BAL showed an absolute increase by day 2 in CD3$^+$ T lymphocytes, including both CD4$^+$ and CD8$^+$ subpopulations (Figure 9, A and B). BAL Tregs (CD3$^+$CD4$^+$CD25$^+$CD127^{lo}Foxp3$^+$) increased approximately 10-fold from day 0 to day 2 after ALI onset. Treg percentages and absolute numbers did not change in peripheral blood (Figure 9, A and C). Patient 2 was a 41-year-old man who developed acute severe pancreatitis complicated by ALI. He was not enrolled until 5 days after the onset of ALI. Compared with patient 1, patient 2 had an increased number of Tregs at enrollment (day 5 after ALI onset), followed by a decline by day 7 after ALI onset (Figure 9B). In contrast, the absolute number of blood Tregs in patient 2 increased over time (Figure 9C). These findings indicate that Tregs are present in the alveolar compartment of humans with ALI and that Treg numbers are dynamically regulated.

Discussion

To our knowledge, the roles of innate and/or adaptive immune pathways in resolution of ALI have not been previously described. Indeed, compared with the wealth of investigation of early steps in the pathogenesis of injury, very little is known in general about mechanisms that determine resolution (1). In this report, we identified that CD4$^+$CD25$^+$Foxp3$^+$ Tregs serve a fundamental role in mediating resolution of lung injury by modulating innate immune responses.

No single animal model reproduces all of the complex characteristics of ALI in humans. We chose to study LPS-induced responses for several reasons. First, this model has been widely used to examine lung injury, and numerous components of the response, particularly acute pathways, have been extensively characterized and are highly reproducible (39–41). Second, LPS, a potent activator of innate immune pathways, can produce diffuse lung injury without prohibitive mortality, greatly facilitating a focused evaluation on resolution of ALI.

Morris observed a recruitment of T cells during murine LPS-induced lung inflammation (42), but concluded that these cells were not critically involved in a model of mild lung injury induced by i.n. LPS (1 μg/mg mouse). The results of our present studies indicate that lymphocytes did not play a major role in the pathogenesis of injury, because the severity of injury 4 days after LPS (as assessed by BAL cell counts, BAL protein, and lung histology) was similar between WT and *Rag-1*$^{-/-}$ mice. In contrast, resolution of ALI in both WT and *Rag-1*$^{-/-}$ mice was determined by the presence or absence of Tregs.

The transcription factor Foxp3 is the best-established marker for defining Tregs, particularly in mice (13, 43, 44), and is thought to play an essential role in generation of suppressive function (44, 45). Wan and Flavell elegantly showed that reduction of Foxp3 in Foxp3-IRES-luciferase-IRES-eGFP (FILIG) mice produced an aggressive autoimmune syndrome, with altered Treg surface properties and impaired Treg-suppressive activity (46). A spontaneous scurfy *Foxp3* gene mutation in mice produces a fatal autoimmune lymphoproliferative disease (47). Similarly, humans with mutations in *FOXP3* develop the clinical syndrome immunodysregulation, polyendocrinopathy and enteropathy, X-linked syndrome (IPEX; ref. 48), and decreased FOXP3 expression has been associated with human diseases (49–51).

In WT mice, we detected CD4$^+$CD25$^+$Foxp3$^+$ Tregs in the alveolar compartment as early as 24–48 hours after exposure to i.t. LPS, after which Treg numbers increased and remained elevated through day 10. The relative extent to which the increase in alveolar Tregs represents recruitment, proliferation, or a combination of the two is presently unknown, although preliminary studies indicate loss of CFSE signal in the BAL by day 7 after transfer of CFSE-labeled Tregs into injured *Rag-1*$^{-/-}$ mice, suggestive of not only alveolar recruitment, but also active proliferation (F.R. D'Alessio and L.S. King, unpublished observation). Tregs have been shown to migrate to inflamed tissues, infectious sites, and tumor microenvironments (52), and we observed enrichment of Tregs in BAL fluid of injured mice. The percentage of alveolar CD4$^+$CD25$^+$ cells that were Foxp3$^+$ decreased after LPS-induced injury and inflammation. Although influx of activated CD4$^+$ cells expressing CD25 contributed to the observed decrease in the percentage of Foxp3$^+$ cells, we believe the changes in percent cells expressing Foxp3 reflect more than simply the influx of activated T cells. First, when purified Tregs from WT spleen (90%–95% Foxp3$^+$) were transferred into *Rag-1*$^{-/-}$ mice after i.t. LPS, only 30%–40% of alveolar CD4$^+$CD25$^+$ cells harvested on day 4 were Foxp3$^+$, consistent with downregulation of Foxp3 in the inflamed alveolus. Second, our ex vivo studies revealed that when purified Tregs from WT spleen were cultured in the presence of

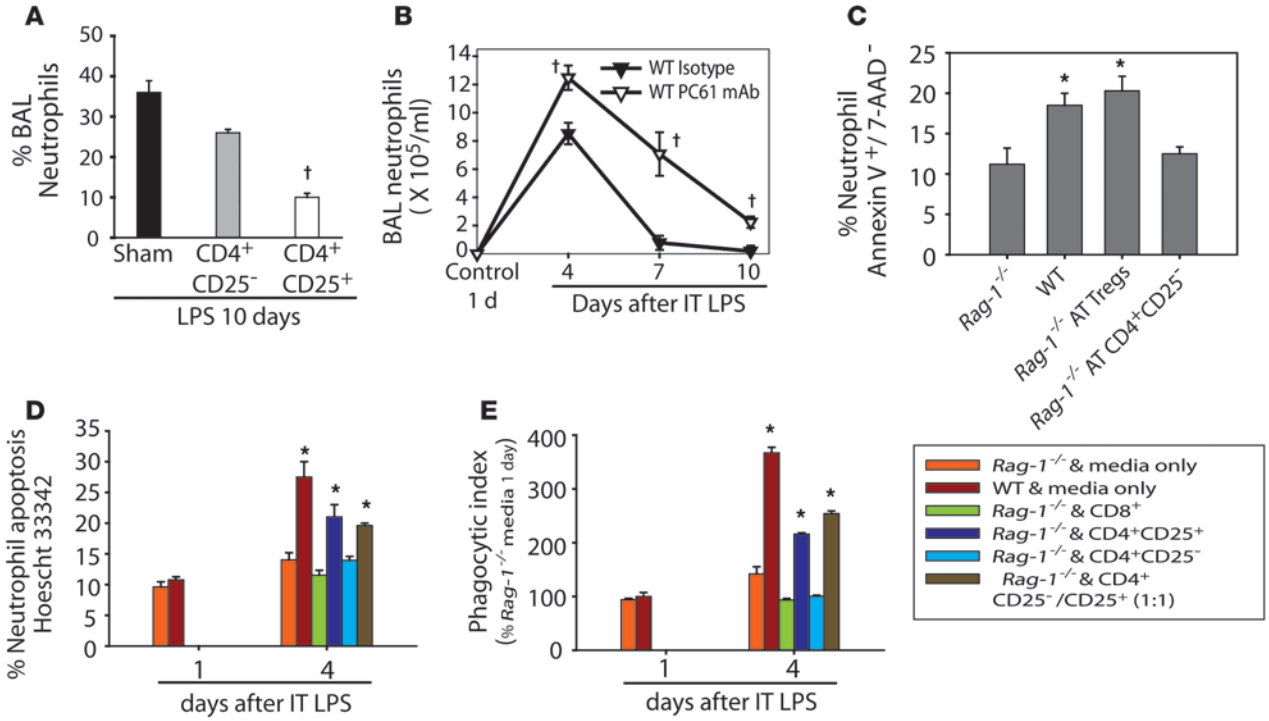

Figure 7

Tregs facilitate alveolar neutrophil clearance in vivo and in vitro. (**A**) After administration of i.t. LPS and AT of PBS sham treatment or the indicated lymphocyte subtypes, the percentage of neutrophils in the BAL on day 10 was assessed. †$P < 0.05$ vs. sham. (**B**) Percent neutrophils in the alveolar compartment of WT mice after receiving isotype or Treg-depleting Abs. †$P < 0.05$ versus isotype Ab. (**C**) Percent BAL neutrophils undergoing apoptosis, as assessed by dual labeling with Annexin V and 7-AAD on day 4 after i.t. LPS in WT or *Rag-1*$^{-/-}$ mice receiving PBS or AT of Tregs or $CD4^+CD25^-$ cells. (**D**) WT and *Rag-1*$^{-/-}$ mice were exposed to i.t. LPS, and on day 1 or day 4, both BAL and ex vivo BAL mixed cultures were performed. Neutrophils and macrophages were cultured in vitro for 6 hours, then media or the indicated lymphocyte subset was added in a 1:10 lymphocyte/macrophage ratio. (**E**) Neutrophil apoptosis or macrophage phagocytosis was assessed 24 hours after addition of the indicated cells in vitro. *$P < 0.05$ vs. day-1 *Rag-1*$^{-/-}$ and media only.

LPS and macrophages, both Foxp3 and FR4 — a highly expressed surface marker in natural Tregs that can be effectively targeted by Ab to mediate Treg depletion (25, 53) — were reduced within 24 hours. Mechanisms underlying this downregulation are not yet known, although IL-6, which is highly abundant in the alveolar compartment of injured mice and released from LPS-stimulated macrophages, has been shown to downregulate Foxp3 expression in natural Tregs (54, 55).

In addition to defining Tregs by phenotypic markers, we found using both in vivo and in vitro studies that these cells exhibit suppressive function. Despite containing only 50% $Foxp3^+$ cells, $CD4^+CD25^+$ cells sorted from the alveolar compartment of WT mice on day 4 after i.t. LPS suppressed proliferation of stimulated responder $CD4^+CD25^-$ cells as effectively as did natural Tregs isolated from naive spleen. This is consistent with the findings of Caramalho, who demonstrated that LPS can increase Treg suppressor efficiency (56); changes in Foxp3 expression after LPS were not assessed in that report. In vivo, we found that Tregs abrogated lung inflammation in *Rag-1*$^{-/-}$ mice in which no other lymphocytes were present, strongly indicating Treg effects on nonlymphoid cells.

In our model, resolution of ALI is achieved by Treg-mediated modulation of innate immune responses in the lung. After transfer of Tregs (but not $CD4^+CD25^-$ cells) into *Rag-1*$^{-/-}$ mice, proinflammatory cytokines decreased and TGF-β doubled. These changes occurred as early as day 4 after injury, coinciding with a significant increase in alveolar Tregs. Similarly, Treg-depleted WT mice had elevated proinflammatory cytokine levels and reduced TGF-β compared with isotype Ab–treated WT mice. Given that the absolute number of BAL Tregs represents less than 0.01% of the total alveolar cells at any point, we hypothesized that Tregs interact with alveolar macrophages— which are abundant in number at all times — to mediate resolution. Alveolar macrophages play a critical role in innate immune responses in the lung, through their ability to recognize pathogens by way of Toll-like receptors as well as through their capacity to produce a wide range of pro- or antiinflammatory mediators and chemokines, to phagocytose apoptotic neutrophils, and to kill bacteria. Macrophages participate in the initiation of inflammatory responses (classically activated, M1 macrophage) as well as resolution of these responses (alternatively activated, M2 macrophage; refs. 57, 58). Our coculture studies demonstrate that Tregs can abrogate LPS-induced TNF-α production from isolated alveolar macrophages in a contact-dependent manner. Coupled with reports of Treg-mediated effects on dendritic cell function (59, 60), our findings strongly indicate cross-talk between innate and adaptive immune systems in regulating the inflammatory environment in the lung after injury.

Further evidence of Treg-mediated modulation of innate immune responses in the lung derived from analysis of alveolar neutrophil dynamics. Apoptosis of inflammatory cells is fundamental to resolution of inflammation, and failure to clear these

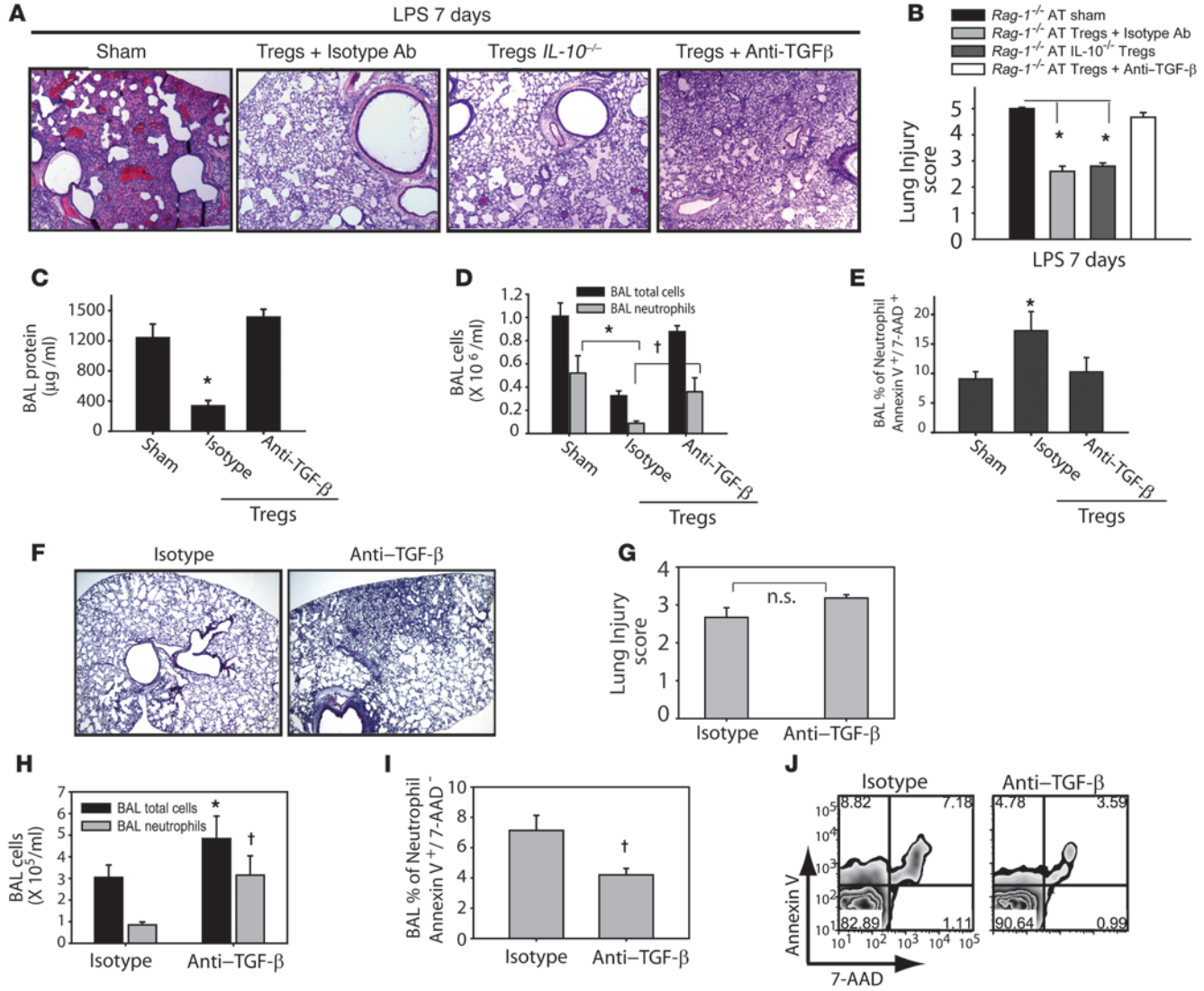

Figure 8

TGF-β blockade abrogates Treg-mediated effects on resolution of lung injury. PBS sham treatment or AT of 1 x 10^6 Tregs (isolated from WT or *IL-10*$^{-/-}$ mice) was performed via tail vein injection (day 0) into i.t. LPS–injured *Rag-1*$^{-/-}$ mice. Anti–TGF-β Ab (150 μg/dose per mouse on days 0 and 4) or isotype Ab were administered. (**A**) H&E stain of representative lung sections on day 7 after i.t. LPS (n = 5 per group). Original magnification, ×40. (**B**) Mean histopathological lung injury scores (n = 4 per group). (**C**–**E**) BAL total protein (**C**) and total cell counts (**D**) were determined for groups as designated. BAL neutrophil apoptosis (**E**) was measured by flow cytometry using dual labeling with Annexin V/ 7-AAD. n = 10 per group. (**F**) Anti–TGF-β or isotype Abs were administered to WT mice on days 0, 2, and 4 after i.t. LPS, and lung histology was examined on day 7. Original magnification, ×20. (**G**) Mean histopathological lung injury scores for samples from **F** (n = 4 per group). P = 0.1. (**H**) BAL total cell and neutrophil counts. (**I** and **J**) After gating on Ly6G cells, decreased BAL neutrophil apoptosis was observed by staining with Annexin V and 7-AAD. (**J**) Flow cytometry of Ly6G$^+$ cells (neutrophils) labeled with Annexin V and 7-AAD. Numbers within plots denote the percentage of cells in the respective quadrants. *P < 0.05 versus respective sham control; †P < 0.05 versus respective isotype control.

cells leads to excessive tissue damage and sustained injury (3, 61). We found that in the absence of Tregs in both *Rag-1*$^{-/-}$ and WT mice, alveolar neutrophils persisted after LPS, and neutrophil apoptosis was reduced. The observed increase in neutrophil number did not appear to result from increased neutrophil chemotactic signals, although we cannot definitively rule out the contribution of an unidentified chemotactic signal. Rather, we demonstrated that when Tregs were present, both in vivo and in vitro, neutrophil apoptosis was increased, consistent with recent reports of findings in vitro (15, 24). Additionally, macrophage efferocytosis was enhanced in the presence of Tregs, supporting the role of these cells in neutrophil clearance. Moreover, phagocytosis of neutrophils by macrophages induces TGF-β1 secretion, resulting in accelerated resolution of inflammation, as previously described (32). Treg-mediated neutrophil apoptosis can result from multiple mechanisms, and studies are ongoing to define these pathways in our model.

TGF-β can have pleiotropic effects in different contexts, including as a potent regulator of the immune and inflammatory systems (62). Disruption of the gene encoding TGF-β in mice pro-

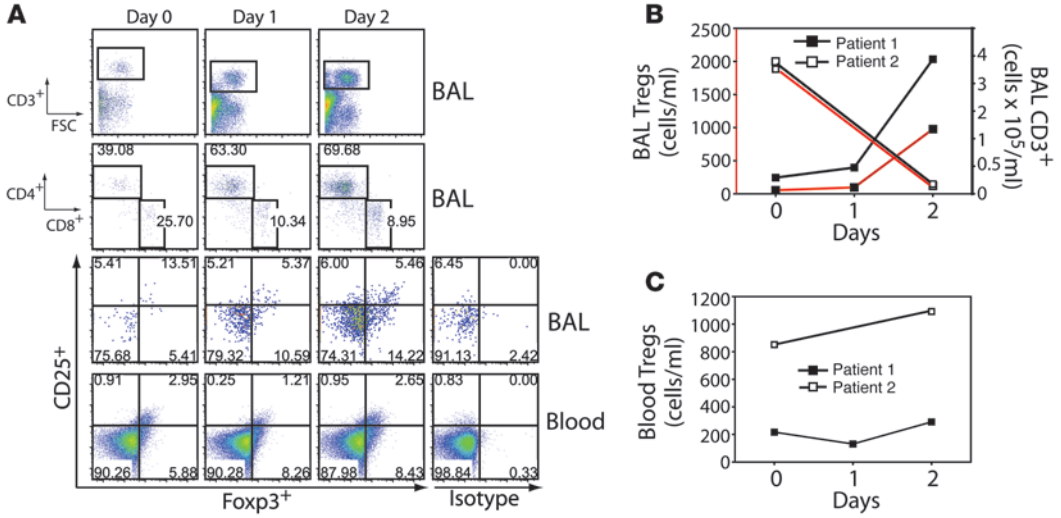

Figure 9

Alveolar Tregs are present in humans with ALI. Mini-BAL and blood sampling was performed on days 0, 1, and 2 relative to enrollment. (**A**) Patient 1 BAL flow cytometry panels for $CD3^+$, $CD4^+$ and $CD8^+$, and $CD3^+CD4^+CD25^{hi}CD127^{lo}Foxp3^+$ cells, as well as flow cytometry for $CD3^+CD4^+CD25^{hi}CD127^{lo}Foxp3^+$ cells in the blood compartment. Intracellular staining with human isotype control Ab for FoxP3, in cells gated as described above, is also shown. Numbers within plots denote the percentage of cells in the respective quadrants or gated regions. (**B**) Absolute number of $CD3^+CD4^+CD25^{hi}CD127^{lo}Foxp3^+$ Tregs in the BAL (right axis) and blood (left axis) over time in patients with ALI. (**C**) Absolute number of $CD3^+CD4^+CD25^{hi}CD127^{lo}Foxp3^+$ Tregs in the blood of patients with ALI.

duces multifocal inflammatory cell infiltration and multiorgan failure (63). In response to bleomycin, TGF-β plays a critical role in the resolution of lung tissue injury (64). However, TGF-β may also have harmful effects in different contexts (65). Sustained elevation of TGF-β has been linked to autoimmune disorders, susceptibility to opportunistic infections, and fibrotic complications of chronic inflammatory conditions (62), and TGF-β increased alveolar epithelial permeability by a mechanism that involved depletion of intracellular glutathione (66). We believe a tightly regulated increase of TGF-β at sites of inflammation is important for resolution of lung injury.

In our studies, TGF-β in BAL fluid increased on day 4 after LPS when Tregs were present. We could not detect secretion of TGF-β by Tregs, nor could we detect cell surface expression of the TGF-β–associated marker LAP in Tregs from the BAL of LPS-challenged mice or in cocultures of LPS-activated macrophages and Tregs. This is not entirely surprising, because Treg TGF-β expression is upregulated by activation through the TCR (33), a signaling pathway not used by LPS. Consistent with a non-Treg source for TGF-β, alveolar TGF-β was reduced but present in mice even when Tregs were absent, that is, both in Treg-depleted WT mice and in *Rag-1*$^{-/-}$ mice. We found that Tregs boosted macrophage secretion of TGF-β. In addition, Treg-mediated contact-dependent reduction of TNF-α from LPS-stimulated macrophages was lost by inhibition of TGF-β, which suggests cross-talk between innate and adaptive immune cells that drives resolution. Our in vivo and in vitro findings are consistent with in vitro data from Tiemessen et al. showing that human Tregs can induce alternative activation of monocytes and inhibit their proinflammatory response to LPS (67).

The mechanisms underlying suppressive effects of Tregs in vivo appear to be complex (13, 44, 68–70). IL-10–mediated Treg effects have been demonstrated, particularly in antigen-specific responses (71–73). We found that Treg-derived IL-10 was not required to achieve resolution of lung injury after i.t. LPS. Although TGF-β has also been proposed to play a critical role in Treg-mediated suppression (33, 74, 75), recent work indicates that TGF-β may be more important in influencing Treg-suppressive activity and Foxp3 expression (76), rather than as a Treg-derived mediator (77, 78). Consistent with this notion, we were unable to detect either secreted or membrane-bound TGF-β from Tregs after LPS stimulation. Regardless, inhibition of TGF-β abrogated Treg-dependent suppression of macrophage TNF-α production, as well as Treg-mediated resolution of lung injury, in both WT and *Rag-1*$^{-/-}$ mice. Although inhibition of TGF-β in our model altered the inflammatory response and delayed injury resolution, the effect was not as profound as that observed when Tregs were absent. We believe this indicates that Tregs mediate resolution through both TGF-β–dependent and –independent mechanisms. We cannot exclude a contribution from other potential mechanisms of Treg-mediated immunosuppression, such as modulation of dendritic cell function and maturation through cytotoxic T lymphocyte antigen-4 (CTLA-4) or lymphocyte-activation gene 3 (LAG-3); adenosine-mediated immunosuppression by ectoenzymes CD39 and CD73; or suppression by cytolysis through secretion of granzymes (44).

Nakos and colleagues described a general increase in BAL total lymphocytes in patients with ALI for greater than 6 days compared with earlier time points (79). To our knowledge, we are the first to describe the presence of Tregs in the airspaces of humans with ALI. Alveolar Treg numbers dynamically changed during the course of ALI. Longitudinal analysis of Treg abundance and phenotype in larger numbers of patients with ALI is beyond the scope of this initial description, but could prove highly informative in examining the potential contribution of Tregs to resolution of human ALI.

We found that after lung injury with LPS, Tregs migrated to the inflamed alveolar compartment, where they orchestrated a complex series of events, fundamentally driving the transition from

a proinflammatory environment in the alveolus to one favoring resolution and repair. Modulation of innate immune responses, including neutrophil apoptosis, macrophage function, and cytokine profiles, is central to the coordination of this response. Treg-mediated effects ultimately manifest as facilitated resolution of lung injury and improved survival, and reinforce a recent report indicating that adaptive immune cells can play central roles in regulating innate immune pathways (80). Notably, we observed Treg-mediated resolution even when cells were delivered as rescue therapy 24 hours after the onset of ALI, a striking contrast with most experimental interventions for ALI to date.

ALI in critically ill patients is an important clinical problem, accounting for more than 75,000 deaths each year in the United States. No specific therapies are available. To date, the predominant focus of work in this area has been on interruption of early events in disease pathogenesis, with almost no description of potentially distinct mechanisms of resolution. We believe that our work highlights a fundamental role for Tregs in regulating innate immune responses to mediate resolution of ALI.

Methods

Mice. Male C57BL/6 congenic CD45.1 mice, C57BL/6 WT and *Rag-1*$^{-/-}$ mice, and C57BL/6 *IL-10*$^{-/-}$ mice (6–8 weeks old) were purchased from The Jackson Laboratory and housed in a pathogen-free facility. All experiments were conducted under protocols approved by the Johns Hopkins Animal Care and Use Committee.

Mouse preparation. Mice were anesthetized with i.p. ketamine and acetylpromazine (150 and 13.5 mg/kg, respectively) before exposure of the trachea. *Escherichia coli* LPS (O55:B5 Sigma-Aldrich L2880) at 3.75 μg/g mouse or sterile water as control was instilled i.t. via a 20-gauge catheter. At 1, 4, 7, and 10 days after instillation, 8–10 mice per group were anesthetized and killed by exsanguinations from their inferior vena cava.

Analysis of BAL fluid. BAL was obtained by cannulating the trachea with a 20-gauge catheter. The right lung was lavaged twice (each aliquot 0.7 ml; calcium-free PBS); total returns averaged 0.9–1.1 ml/mouse. BAL was routinely cultured; no mice were found to be infected in these studies. BAL was centrifuged at 600 *g* for 8 minutes at 4°C. The cell-free supernatants were stored at –80°C for later analysis. The cell pellet was diluted in PBS, and total cell number was counted with a hemocytometer after staining with trypan blue. Differential counts were done on cytocentrifuge preparations (Cytospin 3; Shandon Scientific) stained with Dif-Quik stain (Baxter Diagnostics), counting 300 cells per sample. Flow cytometry (as described below) of BAL fluid was performed in our initial studies to confirm neutrophil numbers (GR-1 labeling) and closely correlated with our BAL cytospins counts; subsequent evaluation of neutrophil numbers was performed only with cytospin/cell differentials. Total protein was measured in the cell-free supernatant using the method of Lowry (81).

Isolation of lung mononuclear cells. Lungs were minced and incubated at 37°C in an enzyme cocktail of RPMI containing 2.4 mg/ml collagenase I and 20 μg/ml DNase (Invitrogen), then mashed through a 70-μm nylon cell strainer (BD Falcon). A 23% and 70% bilayer Percoll (Amersham Biosciences) gradient was performed, and the interface was later collected.

Lung morphology and lung injury scoring. Lungs from animals (n = 5 per time point) were inflated to 25 cm H_2O with 1% low-melting agarose (Invitrogen) for histologic evaluation by H&E staining (82). Two investigators blinded to group assignments analyzed the samples and determined levels of lung injury according to the semiquantitative scoring outlined below. All lung fields at ×20 magnification were examined for each sample. Assessment of histological lung injury was performed by grading as follows: 1, normal; 2, focal (<50% lung section) interstitial congestion and inflammatory cell infiltration; 3, diffuse (>50% lung section) interstitial congestion and inflammatory cell infiltration; 4, focal (<50% lung section) consolidation and inflammatory cell infiltration; 5, diffuse (>50% lung section) consolidation and inflammatory cell infiltration. The mean score was used for comparison between groups.

Isolation of CD4$^+$*CD25*$^+$ *T cells and CD4*$^+$*CD25*$^-$ *T cells and AT*. Spleens were removed and prepared for single-cell suspensions. CD4$^+$ T cells were isolated from the resulting splenocytes using magnetic bead separation. Briefly, total splenocytes were depleted of CD8 (Ly-2), CD11b (Mac-1), CD45R (B220), CD49b (DX5), Ter-119 cells using biotin-labeled specific mAbs (Miltenyi Biotec), anti-biotin magnetic beads, and an LD magnetic bead column (Miltenyi Biotec). To isolate CD4$^+$CD25$^+$ and CD4$^+$CD25$^-$ T cells, purified CD4$^+$ T cell populations were incubated with PE-labeled anti-CD25 Ab (Miltenyi Biotec) and anti-PE magnetic beads and were isolated by MACS separation column, and CD4$^+$CD25$^-$ T cells were isolated by negative selection using anti-CD25 microbeads. The purity of CD4$^+$, CD4$^+$CD25$^+$, and CD4$^+$CD25$^-$ T cell fractions was always greater than 95%. Purified single-cell suspensions (1×10^6 cells in 100 μl PBS) were adoptively transferred 60 minutes or 24 hours after i.t. LPS via tail vein injection.

Flow cytometry. Cells were incubated with Fc Block-2.4G2 (BD Biosciences — Pharmingen) Ab to block Fcγ III/II receptors before staining with a specific Ab. The following Abs (BD Biosciences — Pharmingen) were used for surface staining: FITC-conjugated anti-CD4 and PE-conjugated anti-CD25, PerCPCy5.5-conjugated anti-CD8, allophycocyanin-conjugated anti-CD3, and respective isotype Abs. For intracellular staining of Foxp3, cells were fixed and permeabilized with Foxp3 staining buffer (eBioscience), then stained with allophycocyanin-conjugated anti-mouse^{Foxp3} mAbs (0.5 μg per 10^6 cells; eBioscience). Lymphocytes were gated with characteristic low forward scatter/side scatter, using a FACSAria instrument and FACSDiva for data acquisition (Becton Dickinson) and Flowjo for analysis (Tree Star Inc.).

Human BAL analysis. We screened patients in the Johns Hopkins Hospital Intensive Care Unit who met previously defined criteria for ALI (19). After securing informed consent, we performed mini-BAL (38), a nonbronchoscopic bedside method of performing a small-volume BAL that involves blind specimen sampling from distal airspaces. Specimens were obtained with the Combicath (Plastimed) catheter. Briefly, the catheter was introduced from its protective sheath into the endotracheal tube through a standard bronchoscopy adapter. It was then gently advanced into a lung until it became wedged in a distal airway. We injected 2 20-ml aliquots of normal saline and a 5-ml air bolus into the lungs. Retrieval of fluid usually averages between 4 and 8 ml. Upon completion of the procedure, the catheter was removed from the endotracheal tube.

Cells were Fc incubated with human IgG (Rockland) to block Fc receptors; surface stained with allophycocyanin-Cy7–conjugated anti-CD3 (SK7; BD Biosciences — Pharmingen), AF700-conjugated anti-CD4 (RPA-T4; BD Biosciences — Pharmingen), PECy7-conjugated anti-CD25 (M-A251; BD Biosciences — Pharmingen), PacOrange-conjugated anti-CD8 (3B5; Invitrogen), and PerCPCy5.5-conjugated anti-CD127 (RDR5; eBioscience); and intracellularly stained with allophycocyanin-conjugated anti-Foxp3 (PCH101; eBioscience). Panel used a UV excitable live dead discrimination assay (Invitrogen). Cells were analyzed on a FACSAria (BD Biosciences) with FloJo software (Tree Star Inc.). All human work was approved by an Institutional Review Board at the Johns Hopkins Hospital.

Measurement of lung homogenate cytokines/chemokines. A mouse cytokine multiplex kit (Mouse Cytokine 10-plex; Bio-Rad Laboratories) was used to assay BAL fluid for GM-CSF, G-CSF, KC, IL-1β, IL-4, IL-13, IL-6, MIP-1α, MCP-1, and IL-12. ELISA kits were used for TNF-α, IL-10, IFN-γ, and active TGF-β in BAL (R&D Systems).

TGF-β neutralization. Pan–TGF-β polyclonal neutralizing Abs (AB-100-NA) and normal rabbit IgG (AB-105-C) were purchased from R&D Systems. Groups of 10 mice received 150 μg per injection per mouse of anti–TGF-β or rabbit IgG as control at days 0 and 4 after LPS and AT, as described previously (74, 83, 84).

In vivo depletion of Tregs. WT animals were given 0.5 mg/dose/mouse i.p. of a depleting CD25 mAb (PC61; BioXcell) or isotype (rat IgG, Sigma-Aldrich) on days –2, 0, 3, and 6 after i.t. LPS challenge. Depletion of $CD4^+CD25^+$ cells was confirmed in spleen and blood by flow cytometry.

In vitro proliferation assays. $CD4^+CD25^-$ cells (5×10^4) from C57BL/6 mice were cultured in 96-well plates (0.2 ml) with 5×10^4 irradiated APCs (T-depleted spleen cells) and 0.5 μg/ml anti-CD3 for 3 days in the presence of varying numbers of Tregs. Proliferation was measured in triplicates by the incorporation of [^{3}H]TdR during the last 8 hours of the coculture. APCs were obtained by negative selection of CD90.2 spleen population using magnetic microbeads (Miltenyi).

Ex vivo BAL cocultures. Cells obtained from BAL, performed 4 days after LPS instillation, were resuspended at 0.5×10^6 cells/ml in RPMI supplemented with 10% FCS and 1% penicillin/streptomycin, and cultured on 8-well tissue culture slides (Fisher Scientific). Duplicate samples were set up, and experiments were repeated twice. After 2 hours, lymphocyte subsets as designated at a lymphocyte/macrophage ratio of 1:10 were added to cultures, and cells were harvested at 24 and 48 hours by gentle scraping. Cytospins were stained with Diff-Quik for determination of phagocytosis of neutrophils by macrophages. Neutrophil apoptosis was determined by Hoechst 33342 staining (10 μg/ml) after brief fixation with methanol.

Peritoneal macrophage cultures. Peritoneal macrophages were lavaged from C57BL/6 WT mice (The Jackson Laboratory) 4 days after injection of 3 ml sterile thioglycollate (Sigma-Aldrich). Cells adhered overnight in RPMI 1640 emented with 10% heat-inactivated low-LPS FBS plus 1% penicillin/streptomycin and 1% glutamine before use.

Neutrophil apoptosis. BAL cells obtained 4 days after LPS were stained for Annexin V and 7-AAD (BD Biosciences) and analyzed by flow cytometer. Neutrophils were identified by Ly6G-FITC (BD Biosciences), and apoptosis was determined by Annexin V^+/7-AAD^- double staining using Flowjo software (Tree Star Inc.).

Statistics. Differences in measured variables between groups at each time point were assessed by 2-tailed unpaired Student's *t* test. Survival curves were analyzed with the log-rank test. Data are expressed as mean ± SEM where applicable. Statistical difference was accepted at *P* values less than 0.05.

Acknowledgments

The authors thank James Watkins for expert assistance with tissue processing for histologic studies; Michael Crow and Priya Kesari (Johns Hopkins Pulmonary Division Cytokine Core) for assistance with the bioplex assay; and Mark Soloski and Joe Chrest for their assistance in the Johns Hopkins Bayview Flow Cytometry Core. This work was supported by NHLBI, NIH, grant HL089346 (to L.S. King) and by NHLBI, NIH, SCCOR in Acute Lung Injury grant P050 HL 073994-01.

Received for publication June 16, 2008, and accepted in revised form July 15, 2009.

Address correspondence to: Landon S. King, Division of Pulmonary and Critical Care Medicine, Johns Hopkins Asthma and Allergy Center, 5501 Hopkins Bayview Circle, Room 4B.71A, Baltimore, Maryland 21224, USA. Phone: (443) 287-3343; Fax: (443) 287-3349; E-mail: lsking@jhmi.edu.

1. Ware, L.B., and Matthay, M.A. 2000. The acute respiratory distress syndrome. *N. Engl. J. Med.* **342**:1334–1349.
2. Rubenfeld, G.D., et al. 2005. Incidence and outcomes of acute lung injury. *N. Engl. J. Med.* **353**:1685–1693.
3. Serhan, C.N., and Savill, J. 2005. Resolution of inflammation: the beginning programs the end. *Nat. Immunol.* **6**:1191–1197.
4. Savill, J. 1997. Apoptosis in resolution of inflammation. *J. Leukoc. Biol.* **61**:375–380.
5. Henson, P.M. 2005. Dampening inflammation. *Nat. Immunol.* **6**:1179–1181.
6. Henson, P.M., and Hume, D.A. 2006. Apoptotic cell removal in development and tissue homeostasis. *Trends Immunol.* **27**:244–250.
7. Ross, R. 1994. The role of T lymphocytes in inflammation. *Proc. Natl. Acad. Sci. U. S. A.* **91**:2879.
8. Olsson, B., et al. 2003. T-cell-mediated cytotoxicity toward platelets in chronic idiopathic thrombocytopenic purpura. *Nat. Med.* **9**:1123–1124.
9. Das, J., et al. 2006. Natural killer T cells and CD8+ T cells are dispensable for T cell-dependent allergic airway inflammation. *Nat. Med.* **12**:1345–1346; author reply 1347.
10. Hotchkiss, R.S., et al. 2000. Caspase inhibitors improve survival in sepsis: a critical role of the lymphocyte. *Nat. Immunol.* **1**:496–501.
11. Sakaguchi, S. 2005. Naturally arising Foxp3-expressing CD25+CD4+ regulatory T cells in immunological tolerance to self and non-self. *Nat. Immunol.* **6**:345–352.
12. Miyara, M., and Sakaguchi, S. 2007. Natural regulatory T cells: mechanisms of suppression. *Trends Mol. Med.* **13**:108–116.
13. Shevach, E.M. 2002. CD4+ CD25+ suppressor T cells: more questions than answers. *Nat. Rev. Immunol.* **2**:389–400.
14. Murphy, T.J., Ni Choileain, N., Zang, Y., Mannick, J.A., and Lederer, J.A. 2005. CD4+CD25+ regulatory T cells control innate immune reactivity after injury. *J. Immunol.* **174**:2957–2963.
15. Montagnoli, C., et al. 2006. Immunity and tolerance to Aspergillus involve functionally distinct regulatory T cells and tryptophan catabolism. *J. Immunol.* **176**:1712–1723.
16. McKinley, L., et al. 2006. Regulatory T cells dampen pulmonary inflammation and lung injury in an animal model of pneumocystis pneumonia. *J. Immunol.* **177**:6215–6226.
17. Mombaerts, P., et al. 1992. RAG-1-deficient mice have no mature B and T lymphocytes. *Cell.* **68**:869–877.
18. Artigas, A., et al. 1998. The American-European Consensus Conference on ARDS, part 2: Ventilatory, pharmacologic, supportive therapy, study design strategies, and issues related to recovery and remodeling. Acute respiratory distress syndrome. *Am. J. Respir. Crit. Care Med.* **157**:1332–1347.
19. Bernard, G.R., et al. 1994. The American-European Consensus Conference on ARDS. Definitions, mechanisms, relevant outcomes, and clinical trial coordination. *Am. J. Respir. Crit. Care Med.* **149**:818–824.
20. Uhlig, H.H., et al. 2006. Characterization of Foxp3+CD4+CD25+ and IL-10-secreting CD4+CD25+ T cells during cure of colitis. *J. Immunol.* **177**:5852–5860.
21. Tarbell, K.V., Yamazaki, S., Olson, K., Toy, P., and Steinman, R.M. 2004. CD25+ CD4+ T cells, expanded with dendritic cells presenting a single autoantigenic peptide, suppress autoimmune diabetes. *J. Exp. Med.* **199**:1467–1477.
22. Lewkowich, I.P., et al. 2005. CD4+CD25+ T cells protect against experimentally induced asthma and alter pulmonary dendritic cell phenotype and function. *J. Exp. Med.* **202**:1549–1561.
23. Campbell, D.J., and Ziegler, S.F. 2007. FOXP3 modifies the phenotypic and functional properties of regulatory T cells. *Nat. Rev. Immunol.* **7**:305–310.
24. Lewkowicz, P., Lewkowicz, N., Sasiak, A., and Tchorzewski, H. 2006. Lipopolysaccharide-activated CD4+CD25+ T regulatory cells inhibit neutrophil function and promote their apoptosis and death. *J. Immunol.* **177**:7155–7163.
25. Yamaguchi, T., et al. 2007. Control of immune responses by antigen-specific regulatory T cells expressing the folate receptor. *Immunity.* **27**:145–159.
26. Thornton, A.M., and Shevach, E.M. 1998. CD4+CD25+ immunoregulatory T cells suppress polyclonal T cell activation in vitro by inhibiting interleukin 2 production. *J. Exp. Med.* **188**:287–296.
27. McGeachy, M.J., Stephens, L.A., and Anderton, S.M. 2005. Natural recovery and protection from autoimmune encephalomyelitis: contribution of CD4+CD25+ regulatory cells within the central nervous system. *J. Immunol.* **175**:3025–3032.
28. Sutmuller, R.P., et al. 2001. Synergism of cytotoxic T lymphocyte-associated antigen 4 blockade and depletion of CD25(+) regulatory T cells in antitumor therapy reveals alternative pathways for suppression of autoreactive cytotoxic T lymphocyte responses. *J. Exp. Med.* **194**:823–832.
29. Teder, P., et al. 2002. Resolution of lung inflammation by CD44. *Science.* **296**:155–158.
30. Miyake, Y., et al. 2007. Protective role of macrophages in noninflammatory lung injury caused by selective ablation of alveolar epithelial type II cells. *J. Immunol.* **178**:5001–5009.
31. Nunes, I., Shapiro, R.L., and Rifkin, D.B. 1995. Characterization of latent TGF-beta activation by murine peritoneal macrophages. *J. Immunol.* **155**:1450–1459.
32. Huynh, M.L., Fadok, V.A., and Henson, P.M. 2002.

Phosphatidylserine-dependent ingestion of apoptotic cells promotes TGF-beta1 secretion and the resolution of inflammation. *J. Clin. Invest.* **109**:41–50.
33. Nakamura, K., et al. 2004. TGF-beta 1 plays an important role in the mechanism of CD4+CD25+ regulatory T cell activity in both humans and mice. *J. Immunol.* **172**:834–842.
34. Savill, J.S., et al. 1989. Macrophage phagocytosis of aging neutrophils in inflammation. Programmed cell death in the neutrophil leads to its recognition by macrophages. *J. Clin. Invest.* **83**:865–875.
35. Matute-Bello, G., and Martin, T.R. 2003. Science review: apoptosis in acute lung injury. *Crit. Care.* **7**:355–358.
36. Groux, H., et al. 1997. A CD4+ T-cell subset inhibits antigen-specific T-cell responses and prevents colitis. *Nature.* **389**:737–742.
37. Liesz, A., et al. 2009. Regulatory T cells are key cerebroprotective immunomodulators in acute experimental stroke. *Nat. Med.* **15**:192–199.
38. Kollef, M.H., Bock, K.R., Richards, R.D., and Hearns, M.L. 1995. The safety and diagnostic accuracy of minibronchoalveolar lavage in patients with suspected ventilator-associated pneumonia. *Ann. Intern. Med.* **122**:743–748.
39. Mei, S.H., et al. 2007. Prevention of LPS-induced acute lung injury in mice by mesenchymal stem cells overexpressing angiopoietin 1. *PLoS Med.* **4**:e269.
40. Rojas, M., Woods, C.R., Mora, A.L., Xu, J., and Brigham, K.L. 2005. Endotoxin-induced lung injury in mice: structural, functional, and biochemical responses. *Am. J. Physiol. Lung Cell Mol. Physiol.* **288**:L333–L341.
41. Ulich, T.R., et al. 1991. The intratracheal administration of endotoxin and cytokines. I. Characterization of LPS-induced IL-1 and TNF mRNA expression and the LPS-, IL-1-, and TNF-induced inflammatory infiltrate. *Am. J. Pathol.* **138**:1485–1496.
42. Morris, P.E., Glass, J., Cross, R., and Cohen, D.A. 1997. Role of T-lymphocytes in the resolution of endotoxin-induced lung injury. *Inflammation.* **21**:269–278.
43. Shevach, E.M., et al. 2006. The lifestyle of naturally occurring CD4+ CD25+ Foxp3+ regulatory T cells. *Immunol. Rev.* **212**:60–73.
44. Vignali, D.A., Collison, L.W., and Workman, C.J. 2008. How regulatory T cells work. *Nat. Rev. Immunol.* **8**:523–532.
45. Sakaguchi, S., Yamaguchi, T., Nomura, T., and Ono, M. 2008. Regulatory T cells and immune tolerance. *Cell.* **133**:775–787.
46. Wan, Y.Y., and Flavell, R.A. 2007. Regulatory T-cell functions are subverted and converted owing to attenuated Foxp3 expression. *Nature.* **445**:766–770.
47. Godfrey, V.L., Wilkinson, J.E., and Russell, L.B. 1991. X-linked lymphoreticular disease in the scurfy (sf) mutant mouse. *Am. J. Pathol.* **138**:1379–1387.
48. Bennett, C.L., et al. 2001. The immune dysregulation, polyendocrinopathy, enteropathy, X-linked syndrome (IPEX) is caused by mutations of FOXP3. *Nat. Genet.* **27**:20–21.
49. Miura, Y., et al. 2004. Association of Foxp3 regulatory gene expression with graft-versus-host disease. *Blood.* **104**:2187–2193.
50. Balandina, A., Lecart, S., Dartevelle, P., Saoudi, A., and Berrih-Aknin, S. 2005. Functional defect of regulatory CD4(+)CD25+ T cells in the thymus of patients with autoimmune myasthenia gravis. *Blood.* **105**:735–741.
51. Huan, J., et al. 2005. Decreased FOXP3 levels in multiple sclerosis patients. *J. Neurosci. Res.* **81**:45–52.
52. Belkaid, Y., and Rouse, B.T. 2005. Natural regulatory T cells in infectious disease. *Nat. Immunol.* **6**:353–360.
53. Walker, L.S. 2007. Regulatory T cells: Folate receptor 4: a new handle on regulation and memory? *Immunol. Cell Biol.* **85**:506–507.
54. Zheng, S.G., Wang, J., and Horwitz, D.A. 2008. Cutting edge: Foxp3+CD4+CD25+ regulatory T cells induced by IL-2 and TGF-beta are resistant to Th17 conversion by IL-6. *J. Immunol.* **180**:7112–7116.
55. Samanta, A., et al. 2008. TGF-beta and IL-6 signals modulate chromatin binding and promoter occupancy by acetylated FOXP3. *Proc. Natl. Acad. Sci. U. S. A.* **105**:14023–14027.
56. Caramalho, I., et al. 2003. Regulatory T cells selectively express toll-like receptors and are activated by lipopolysaccharide. *J. Exp. Med.* **197**:403–411.
57. Goerdt, S., and Orfanos, C.E. 1999. Other functions, other genes: alternative activation of antigen-presenting cells. *Immunity.* **10**:137–142.
58. Gordon, S. 2003. Alternative activation of macrophages. *Nat. Rev. Immunol.* **3**:23–35.
59. Houot, R., Perrot, I., Garcia, E., Durand, I., and Lebecque, S. 2006. Human CD4+CD25high regulatory T cells modulate myeloid but not plasmacytoid dendritic cells activation. *J. Immunol.* **176**:5293–5298.
60. Oldenhove, G., et al. 2003. CD4+ CD25+ regulatory T cells control T helper cell type 1 responses to foreign antigens induced by mature dendritic cells in vivo. *J. Exp. Med.* **198**:259–266.
61. Savill, J., Dransfield, I., Gregory, C., and Haslett, C. 2002. A blast from the past: clearance of apoptotic cells regulates immune responses. *Nat. Rev. Immunol.* **2**:965–975.
62. Letterio, J.J., and Roberts, A.B. 1998. Regulation of immune responses by TGF-beta. *Annu. Rev. Immunol.* **16**:137–161.
63. Shull, M.M., et al. 1992. Targeted disruption of the mouse transforming growth factor-beta 1 gene results in multifocal inflammatory disease. *Nature.* **359**:693–699.
64. Giri, S.N., Hyde, D.M., and Hollinger, M.A. 1993. Effect of antibody to transforming growth factor beta on bleomycin induced accumulation of lung collagen in mice. *Thorax.* **48**:959–966.
65. Kang, H.R., Cho, S.J., Lee, C.G., Homer, R.J., and Elias, J.A. 2007. Transforming growth factor (TGF)-beta1 stimulates pulmonary fibrosis and inflammation via a Bax-dependent, bid-activated pathway that involves matrix metalloproteinase-12. *J. Biol. Chem.* **282**:7723–7732.
66. Pittet, J.F., et al. 2001. TGF-beta is a critical mediator of acute lung injury. *J. Clin. Invest.* **107**:1537–1544.
67. Tiemessen, M.M., et al. 2007. CD4+CD25+Foxp3+ regulatory T cells induce alternative activation of human monocytes/macrophages. *Proc. Natl. Acad. Sci. U. S. A.* **104**:19446–19451.
68. Jonuleit, H., and Schmitt, E. 2003. The regulatory T cell family: distinct subsets and their interrelations. *J. Immunol.* **171**:6323–6327.
69. Weiner, H.L. 2001. The mucosal milieu creates tolerogenic dendritic cells and T(R)1 and T(H)3 regulatory cells. *Nat. Immunol.* **2**:671–672.
70. Fuss, I.J., Boirivant, M., Lacy, B., and Strober, W. 2002. The interrelated roles of TGF-beta and IL-10 in the regulation of experimental colitis. *J. Immunol.* **168**:900–908.
71. Hawrylowicz, C.M., and O'Garra, A. 2005. Potential role of interleukin-10-secreting regulatory T cells in allergy and asthma. *Nat. Rev. Immunol.* **5**:271–283.
72. Meiler, F., et al. 2008. In vivo switch to IL-10-secreting T regulatory cells in high dose allergen exposure. *J. Exp. Med.* **205**:2887–2898.
73. Rubtsov, Y.P., et al. 2008. Regulatory T cell-derived interleukin-10 limits inflammation at environmental interfaces. *Immunity.* **28**:546–558.
74. Marie, J.C., Letterio, J.J., Gavin, M., and Rudensky, A.Y. 2005. TGF-beta1 maintains suppressor function and Foxp3 expression in CD4+CD25+ regulatory T cells. *J. Exp. Med.* **201**:1061–1067.
75. Nakamura, K., Kitani, A., and Strober, W. 2001. Cell contact-dependent immunosuppression by CD4(+)CD25(+) regulatory T cells is mediated by cell surface-bound transforming growth factor beta. *J. Exp. Med.* **194**:629–644.
76. Rubtsov, Y.P., and Rudensky, A.Y. 2007. TGFbeta signalling in control of T-cell-mediated self-reactivity. *Nat. Rev. Immunol.* **7**:443–453.
77. Li, M.O., Sanjabi, S., and Flavell, R.A. 2006. Transforming growth factor-beta controls development, homeostasis, and tolerance of T cells by regulatory T cell-dependent and -independent mechanisms. *Immunity.* **25**:455–471.
78. Marie, J.C., Liggitt, D., and Rudensky, A.Y. 2006. Cellular mechanisms of fatal early-onset autoimmunity in mice with the T cell-specific targeting of transforming growth factor-beta receptor. *Immunity.* **25**:441–454.
79. Nakos, G., Kitsiouli, E.I., Tsangaris, I., and Lekka, M.E. 1998. Bronchoalveolar lavage fluid characteristics of early intermediate and late phases of ARDS. Alterations in leukocytes, proteins, PAF and surfactant components. *Intensive Care Med.* **24**:296–303.
80. Kim, K.D., et al. 2007. Adaptive immune cells temper initial innate responses. *Nat. Med.* **13**:1248–1252.
81. Peterson, G.L. 1977. A simplification of the protein assay method of Lowry et al. which is more generally applicable. *Anal. Biochem.* **83**:346–356.
82. Halbower, A.C., Mason, R.J., Abman, S.H., and Tuder, R.M. 1994. Agarose infiltration improves morphology of cryostat sections of lung. *Lab. Invest.* **71**:149–153.
83. McCormick, L.L., Zhang, Y., Tootell, E., and Gilliam, A.C. 1999. Anti-TGF-beta treatment prevents skin and lung fibrosis in murine sclerodermatous graft-versus-host disease: a model for human scleroderma. *J. Immunol.* **163**:5693–5699.
84. Yamamoto, T., Takagawa, S., Katayama, I., and Nishioka, K. 1999. Anti-sclerotic effect of transforming growth factor-beta antibody in a mouse model of bleomycin-induced scleroderma. *Clin. Immunol.* **92**:6–13.